EDITOR

Doç. Dr. Aykut DEMİRÇALI

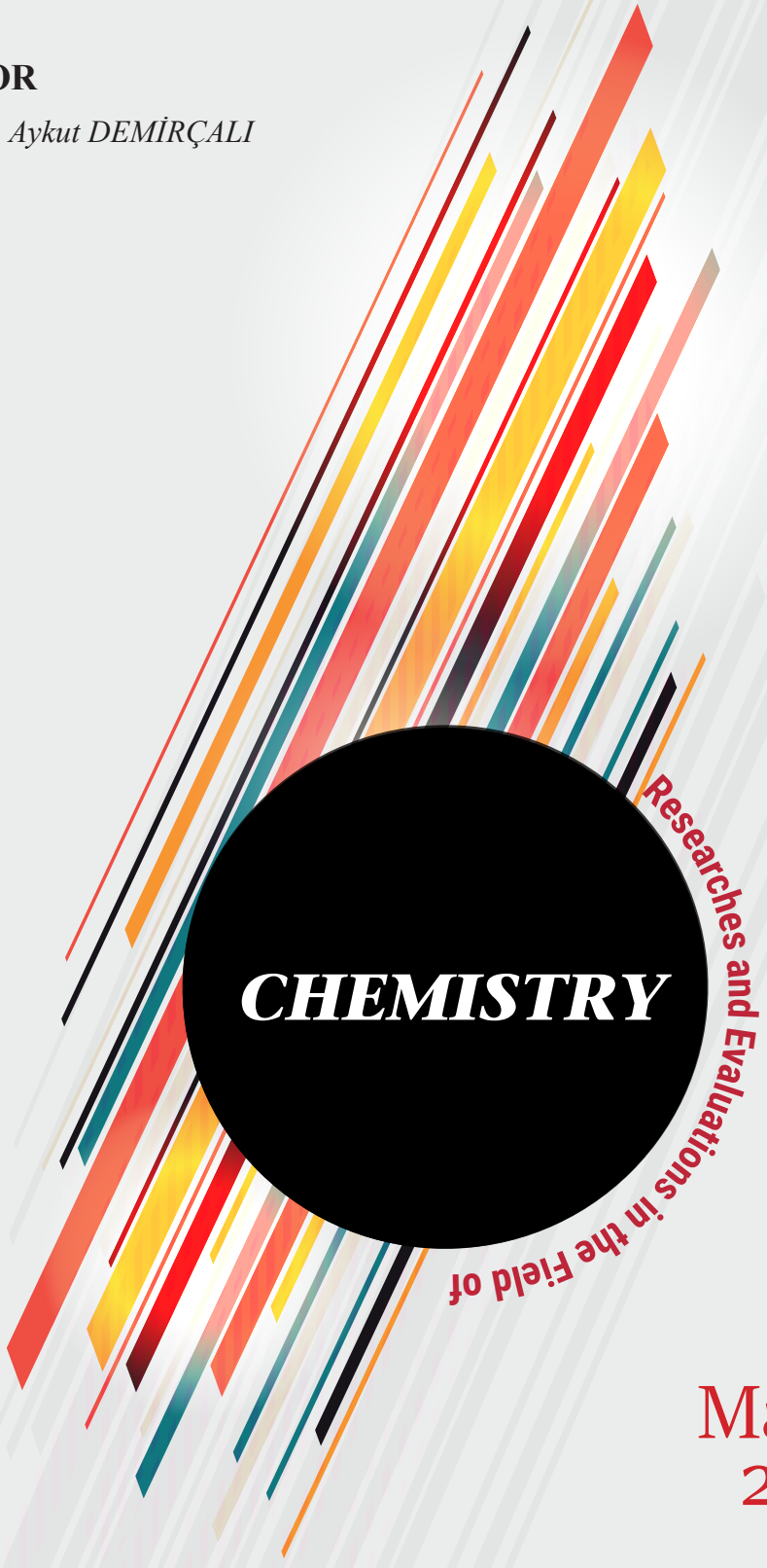

March
2025

İmtiyaz Sahibi • Yaşar Hız
Genel Yayın Yönetmeni • Eda Altunel
Yayına Hazırlayan • Gece Kitaplığı
Editör • Doç. Dr. Aykut DEMİRÇALI

Birinci Basım • Mart 2025 / ANKARA

ISBN • 978-625-388-247-1

Gece Kitaplığı
Adres: Kızılay Mah. Fevzi Çakmak 1. Sokak Ümit Apt
No: 22/A Çankaya/ANKARA Tel: 0312 384 80 40

www.gecekitapligi.com
gecekitapligi@gmail.com

Baskı & Cilt
Bizim Buro
Sertifika No: 42488

Research And Evaluations In The Field Of Chemistry

March 2025

Editor:
Doç. Dr. Aykut DEMİRÇALI

İÇİNDEKİLER

CHAPTER 1

LIKE AN AEASY WAY AS TO WALK DOWN THE STREET AND CHEW GUM CONCURRENTLY, CONTRARY TO POPULAR BELIEF: RECOGNITION OF IONIC SPECIES THROUGH THE FLUORESCENT TECHNIQUE

Erkan HALAY[1]

1 Department of Chemistry, Scientific Analysis Technological Application and Research Center, Usak University, 64200 Usak, Turkey; E-mail: erkan.halay@usak.edu.tr; ORCID: 0000-0002-0084-7709

Department of Chemistry and Chemical Processing Technologies, Banaz Vocational School, Usak University, 64500 Usak, Turkey

Introduction

As ionic species, anions and cations are characterized as key substances in our daily life which have been crucial for human beings' physiological and metabolic function along with plenty of industrial processes. Some of those anionic/cationic species ensure growth with their major biological functions/processes such as energy production, immune response, metabolism, cell signalling, oxygen transport, gene expression regulation and important biomolecule syntheses while others exist as undesired contaminants in the environment (Torres-Ocampo & Palmer, 2023; Kumari et al., 2023; Ahmed et al., 2023). At this point, environmental pollution threat has reached up to very important dimensions since the industrial revolution that occurred with the rapid development of human civilization. However, the majority of those hazardous ions have been released into the soil and water supplies by the food, pharmaceutical, electric/battery, paper and textile industries along with metal refineries that are in need of them and have been harming the aquatic life and plants along with human health (Nangare et al., 2023).

When the crucial implications of these ionic substances are evaluated within the beneficial and harmful contexts, it has been of great significance to establish reliable detection techniques to monitor and manage their presence. Therefore, in the last few decades, metal ion recognition in various environments and biological processes has received a great deal of attention from the scientific community. While early and accurate detection of ionic species can help with understanding of metabolic disorders and the role of those species in disease progression in terms of biological systems, otherwise, it also helps ensure compliance with environmental regulations by enabling the application of corrective actions in terms of environmental systems (Fang et al., 2020; Zheng et al., 2020).

Traditional detection techniques like ion chromatography (IC), atomic absorption/emission spectroscopy (AAS/AES), ultraviolet-visible (UV-Vis) spectroscopy, inductively coupled plasma (ICP) spectroscopy along with mass (MS) spectrometry have been widely used for the analyses of ionic species (Zhong et al., 2022). However, these methods often require expensive instrumentation and equipment, extensive sample preparation, and skilled operators (Gupta et al., 2024). Moreover, related techniques are hardly to use for real-time, on-site analysis that is critical for both clinical diagnostics and environmental assessments due to their poor portability and time-consuming testing procedures (Langari et al., 2022). The increasing demand for the detection systems that are sensitive, cost-effective and portable has directed many scientists to investigate alternative techniques/methodologies. Thus, fluorescent spectroscopy has come to the light as a

promising remedy which has offered remarkable low limit of detection and fast response.

In order to bridge the gap with innovative detection methods in this research field, such techniques, particularly those based on fluorescence, are increasingly being developed to address the limitations of traditional methods. These methods provide a powerful tool for tackling challenges in both biological and environmental contexts by enabling selective and sensitive detection of specific ions (Czarnik, 1993; Wu et al., 2017; Fan et al., 2023).

The following part investigates thoroughly the principles, advancements, and applications of fluorescence-based techniques based on certain examples from current studies, highlighting their improvable potential in ionic species detection.

Fundamentals, Fluorescent-Based Sensing Applications for the Detection of Anions and Cations

As light is one of the most fundamental constituent of life in the universe, new opportunities have been revealed in the context of scientific progress with the advances in the understanding and procedures of the light-emitting applications (Mukherjee, 2022). As components that are useful in this direction, a fluorophore is a fluorescent chemical constituent that absorb photons in the ground state and can lead to fluorescence emission in the excited state. In the presence or absence of fluorophoric moiety that typically contain some conjugated aromatic groups, and/or aliphatic/cyclic constituents with several π-bonds which cause conjugation, light is emitted expectedly or unexpectedly by the fluorescent molecules/sensors/probes (Figure 1) (Verdejo et al., 2022).

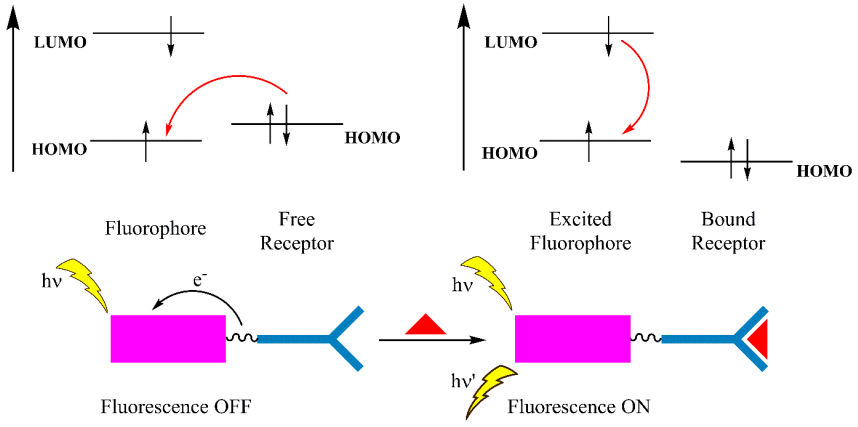

Figure 1. *A specie recognition by a sensor molecule and occurring of emission (adapted from reference Verdejo et al., 2022)*

This fluorescence phenomenon has been leveraged by the fluorescent techniques in order to make qualitative and/or quantitative analyses of specific ions with highly sensitive, selective, and along with simple, quick, cost-effective, efficient detection. The applications of those techniques cover various fields from environmental/industrial process monitoring to medical diagnostics (Kamel et al., 2024; Senthil et al., 2024).

The interaction of light with fluorescent probes/sensors is the key factor for the fluorescence-based detection. These probes/sensors are organic molecules which are designed for emitting light at a specific wavelength upon binding to a target ion. The concentration of the ion with precise quantification could be established through the correlation with the emitted fluorescence. The fluorescent method is useful due to the key features and usefulness of this method include; very high sensitivity and selectivity, rapid response along with short analysis time, real time detection, simplicity of operation, less expensive equipment and non-destructive analysis (Fakayode et al., 2024).

This fluorescence-based technique has offered several advantages when compared to conventional detection methods as follows;

- Sensitivity: That kind of optical analysis method is usually more sensitive with much lower limits of detection and quantification.
- Portability: The sensors/probes produced in this technical context, enable on-site analysis, and that makes them ideal for fieldwork.
- Adaptability: In order to make them work in various environments including aqueous, biological, and solid-phase systems, fluorescent probes can be modified.
- Multiplexing Capability: Enabling simultaneous detection of much more than one (multiple) ionic species by using these fluorescent probes with distinct emission spectra.
- Cost-Effectiveness: Using inexpensive materials by the method and requiring much simpler instrumentation (Fang et al., 2019; Wu and Barner-Kowollik, 2023; Singh et al., 2023).

Until today; in order to detect ionic species, fluorescent organics, inorganic nanoparticles and semiconductor polymer nanoparticles have been developed and have been widely continuing to use, as stated in the literature. Due to their manageable and efficient synthesis, stable luminescence, high sensitivity along with favourable signal/noise ratio, fluorescent organic small molecules attracted

comparatively more attention among those (Yang et al., 2022). Such compounds, especially bearing donor atoms like O-, S- and N- have been more essential thanks to their skill of interacting with numerous metal ions (Mg^{2+}, Cr^{3+}, Mn^{2+}, Fe^{2+}, Fe^{3+}, Co^{2+}, Ni^{2+}, Cu^{2+}, Zn^{2+}, Al^{3+}, Pd^{2+}, Pt^{2+}, Cd^{2+}, Hg^{2+}, Sn^{2+}, Pb^{2+}, Ag^{+}, Au^{3+}, La^{3+}, Ce^{3+}, etc) and anions (F^{-}, Cl^{-}, Br^{-}, I^{-}, SO_4^{2-}, PO_4^{3-}, NO_2^{-}, NO_3^{-}, CN^{-}, etc) (Bin Darwish et al., 2023).

Recent advancements in organic molecular design have significantly enhanced the fluorescence-based detection performance. While fluorescence efficiency is much important for all organic luminescent materials, both the ligand and the metal ion's electronic configuration, along with the structural capacity of the organic sensor for binding to the metal ion, are the parameters that designate the selectivity and the sensitivity of these fluorescent chemosensors (Basheer et al., 2023). In this regard, for the interaction between fluorescent chemosensors and metal ions, various recognition mechanisms have been proposed such as chelation enhanced fluorescence (CHEF), intramolecular charge transfer (ICT), photo-induced electron transfer (PET), fluorescence resonance energy transfer (FRET), excited-state intramolecular proton transfer (ESIPT) and the mechanism of aggregation-induced emission (AIE) (Singh et al., 2023; Park et al., 2020).

The ICT mechanism has been widely utilized toward the detection of both anions and cations. In this mechanism, the fluorophore directly interacts with the receptor, leading to the formation of a push-pull system between electron-rich and electron-poor terminals. Then, when the interaction occurs between the receptor and a specific analyte, the push-pull character has been weakened or enhanced and that causes a shift in wavelength, either to the longer wavelength or the shorter wavelength. In the ESIPT mechanism, excited-state protons are transferred to or from the molecule at various rates before returning to the ground state. This ultrafast process involves the conversion of a hydroxyl or amino proton into a carbonyl O^{-} atom or an imine N^{-} atom. ESIPT-based chemosensors typically exhibit large Stokes' shifts, minimizing interference from other fluorescent molecules in the medium. (Bin Darwish et al., 2023).

Another widely used mechanism in fluorescence sensing, CHEF is described as the binding of a metal ion to a fluorophore causing

increment in fluorescence intensity. This arises from the reduction of non-radiative decay pathways such as rotation and vibration, followingly leading to a stronger fluorescence signal. In fluorescence-based sensing, PET is another fundamental mechanism, where the fluorescence of the fluorophore is adjusted by the electron transfer processes between ligand and the guest. These type of sensors typically serve as "turn-on" or "turn-off" sensing systems in response to metal ion binding. As a non-radiative energy transfer process, FRET occurs when an energy donor fluorophore gives its excitation energy to an acceptor fluorophore in close proximity, adjusting fluorescence emission based on metal-induced structural changes (Formica et al., 2012).

Lastly, but not least, AIE phenomenon was first introduced to the scientific community in 2001 as a unique characteristic of some luminophores. As seen in Figure 2, through the free permitted rotation of the chemical bonds, fluorescence is not emitted by the molecular system or weak fluorescence is emitted in the solution state. However, when the aggregation occurs and so the rotation is prohibited, enhanced fluorescence is generated. By emitting fluorescence only upon binding to a specific guest/ion and thus reducing background noise and improving detection accuracy and sensitivity, this AIE phenomenon overcomes another one, aggregation-caused quenching (ACQ) effect of traditional fluorescent materials which shows turn-off feature wherein the fluorescent quenching in the original emission peak resulted in poor sensitivity (Yang et al., 2022; Suzuki et al., 2020).

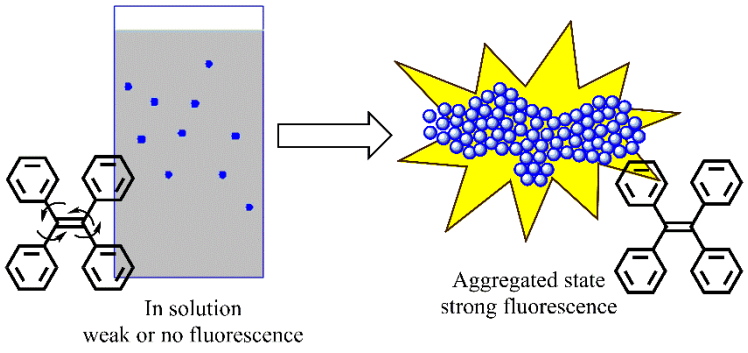

Figure 2. *Status of fluorescence emission in the solution and in the aggregation state.*

In light of the comprehensive information provided above, and on the basis of a number of primary fluorescence mechanisms, the latest progress was trying to be given below through the works of the recent past.

Pawar et al. (2015) reported the design of a new and simple *o*-phenylene diamine derivative having Schiff base feature in order to use the compound for metal ion sensing. As a result of their experiments, they determined that it could be used for dual detection of Cu^{2+} and Ni^{2+} cations selectively over other metal ions (Figure 3). The PET mechanism along with imine C=N isomerization was proposed to explain the superior sensing response of the sensor molecule at the nanomolar level.

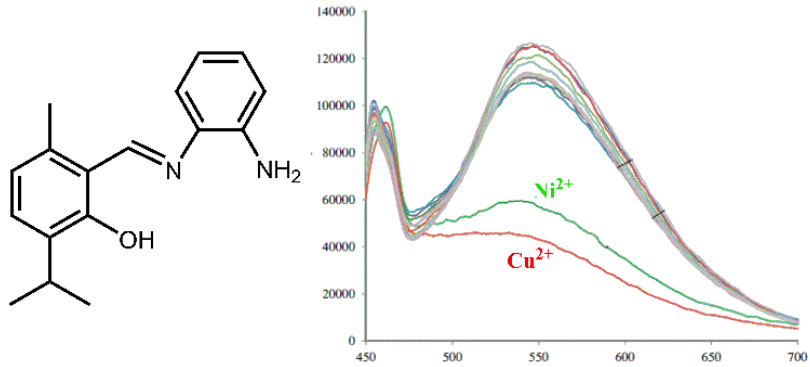

Figure 3. *A Schiff base compound designed as Ni^{2+} and Cu^{2+} fluorescent sensor.*

Xie et al. (2019) introduced a novel probe derived from rhodamine spirolactam and benzothiazole groups as a fluorescent chemosensor for the detection of Cu^{2+}, Co^{2+}, and Ni^{2+} metal ions through distinct recognition process (Figure 4). The related sensor exhibited ratiometric changes and turn-on fluorescence response at 350 and 540 nm, in the presence of those ions. The detection limits were reported as 26 nm, 54 nm and 101 nm for Cu^{2+}, Co^{2+}, and Ni^{2+} respectively by the ratiometric fluorometric measurements, and ESIPT process was found to be responsible for such spectral results.

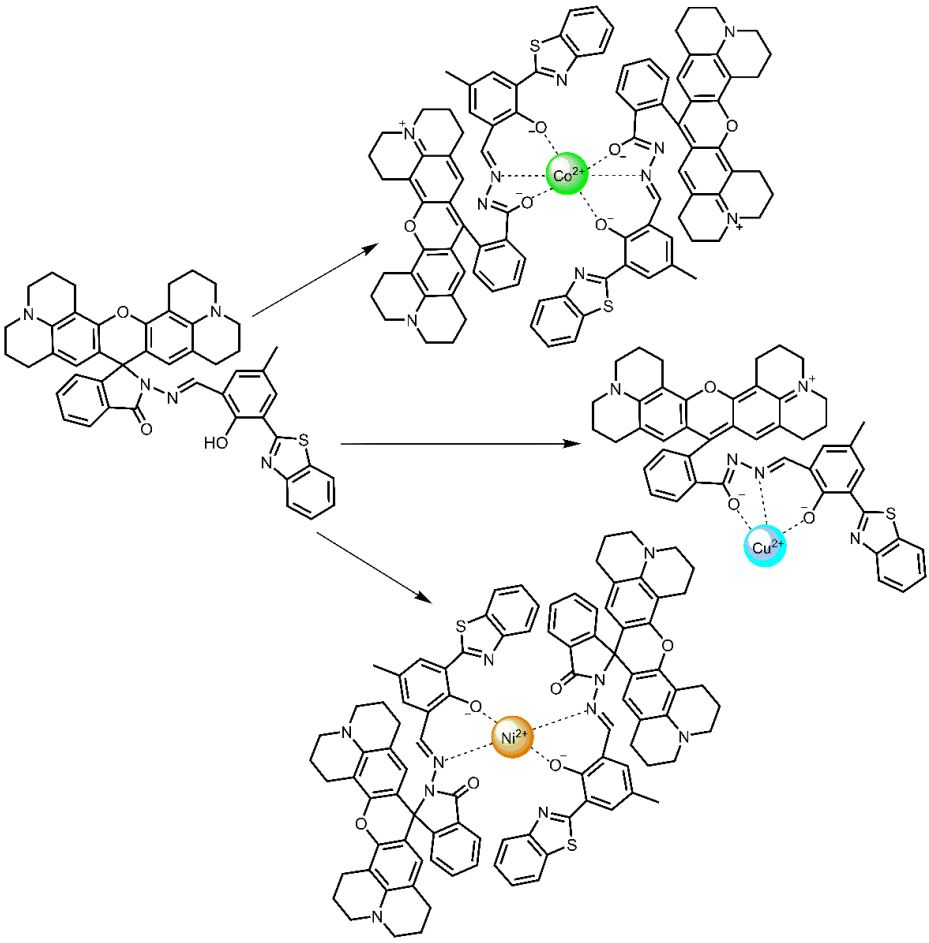

Figure 4. *Sensing of Co^{2+}, Cu^{2+} and Ni^{2+} ions by rhodamine/benzothiazole based sensor.*

Reddy et al. (2021) designed and synthesized cinnamonitrile based naphthalimide-benzothiazole conjugate with the purpose of anion detection (Figure 5). Besides having AIE feature in varying THF/H_2O mixture because of the restricted C-C bond rotation in the molecule, their sensor molecule exhibited turn-on fluorescent characteristic in the presence of CN^- ion with the detection limit value of 33.5 nM.

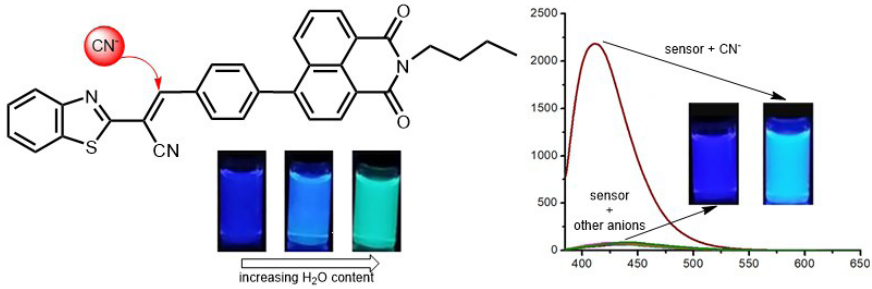

Figure 5. *A naphthalimide-benzothiazole based fluorescent probe for cyanide detection.*

Gu et al. (2019) designed a sensor candidate containing pyrimidine and pyrazole moieties for the applications of metal recognition (Figure 6). They reported that the fluorescent sensor compound could simultaneously detect Cu^{2+} and Ni^{2+} ions in the presence of other metal cations. Upon binding these metals, due to the excited-state energy/charge shifting mechanism, total quenched emission of the related fluorescent sensor was observed along with the low detection limits of 0.043 μM and 0.038 μM for Cu^{2+} and Ni^{2+}, respectively.

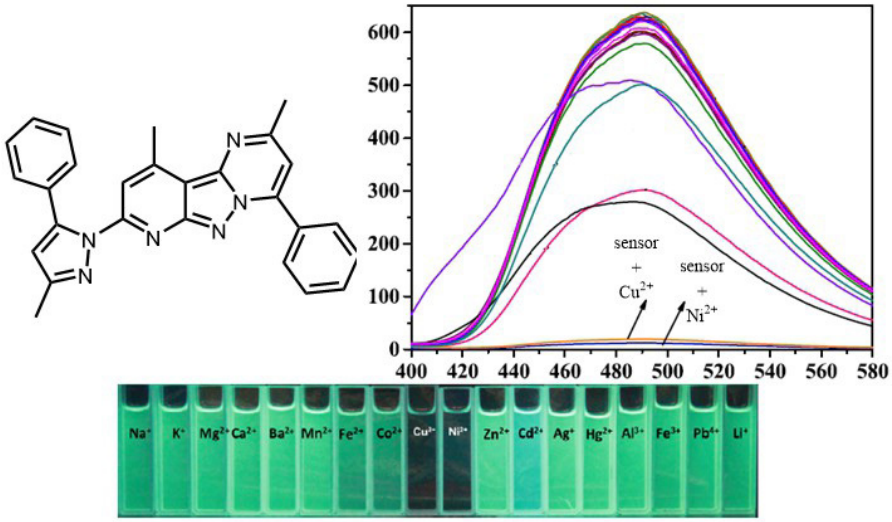

Figure 6. *A fluorescent Cu^{2+}/Ni^{2+} sensor based on pyrazolopyrimidine core.*

Yang et al. (2021) designed and synthesized a new coumarin-based AIE fluorescent sensor candidate. This candidate molecule showed turn-off affinity towards OCl^- ion with fast response and non-negligible detec-

tion limit with the value of 0.32 μM. Additionally, as with many other AIE featured molecules, this coumarin-based sensor showed low fluorescence with the low fraction of water, however, by the increment of water fraction to the 80% value percent a clear and stronger fluorescent emission appeared (Figure 7).

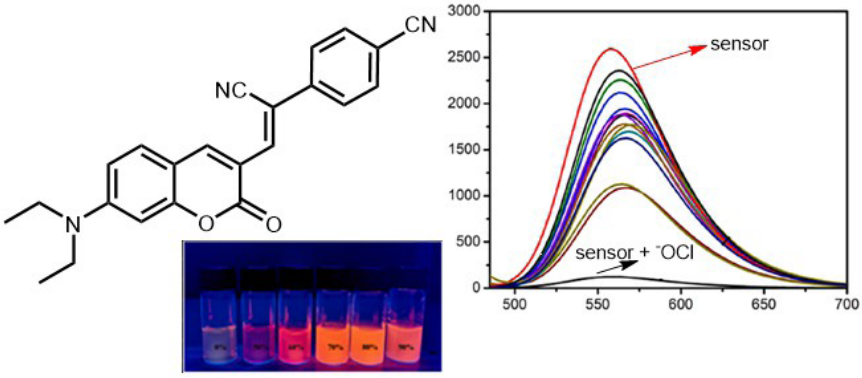

Figure 7. *An AIE sensor based on coumarin scaffold for hypochlorite detection.*

More recently, Kang et al. (2022) developed a tetraphenylethylene analogous ligand containing picolylamine group. The related compound displayed typical AIE properties in THF/H_2O mixture at higher H_2O content possessing high luminous efficiency. In addition, the sensor candidate exhibited binding selectivity for Cu^{2+} ion through an on-off-on fluorescence property and with the detection limit of 35 nM. While Cu^{2+} could bind quickly to the sensor in order to form the ligand-metal complex and caused fluorescence quenching, after that, the addition of PO_4^{3-} anion to the ligand-Cu^{2+} complex showed significant increase in fluorescence intensity (Figure 8). Thus, it revealed that ligand-Cu^{2+} complex could be used as a secondary PO_4^{3-} selective fluorescence sensor with the detection limit of 19 nM.

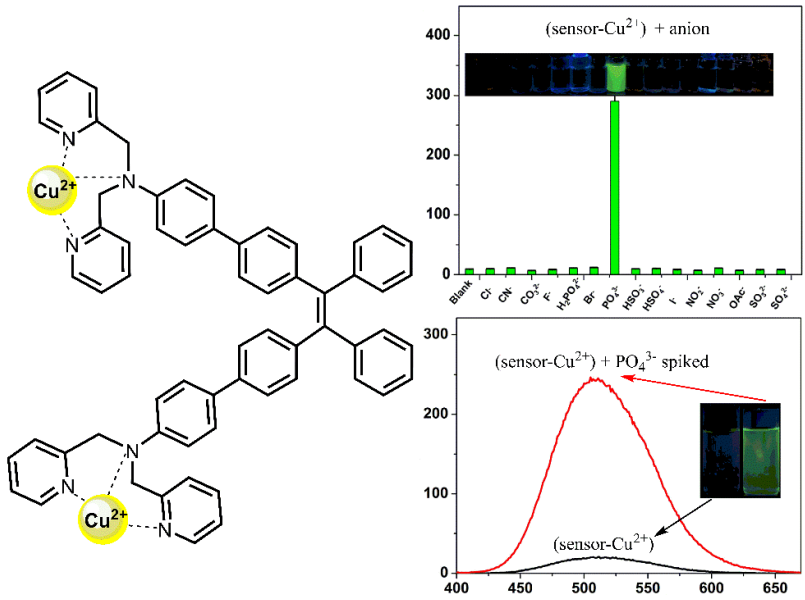

Figure 8. *An AIE featured Cu^{2+}/PO_4^{3-} sensor derived from picolylamine and tetraphenylethylene.*

Turkoglu and Ozturk (2022) reported the synthesis of selenophenothiophene-cored triphenylamine and dimethoxy triphenylamine analogues along with dimesitylborane acceptor unit (Figure 9). As a result of the photophysical properties measurement of both synthesized fluorophores, it was observed that triphenylamine analogue had both AIE and ICT features, however dimethoxy triphenylamine analogue showed ICT mechanism dominant. Through the ion recognition experiments, both analogues showed good responses to anions as F^- and CN^-, with the detection limits of 0.12-2.43 ppm range.

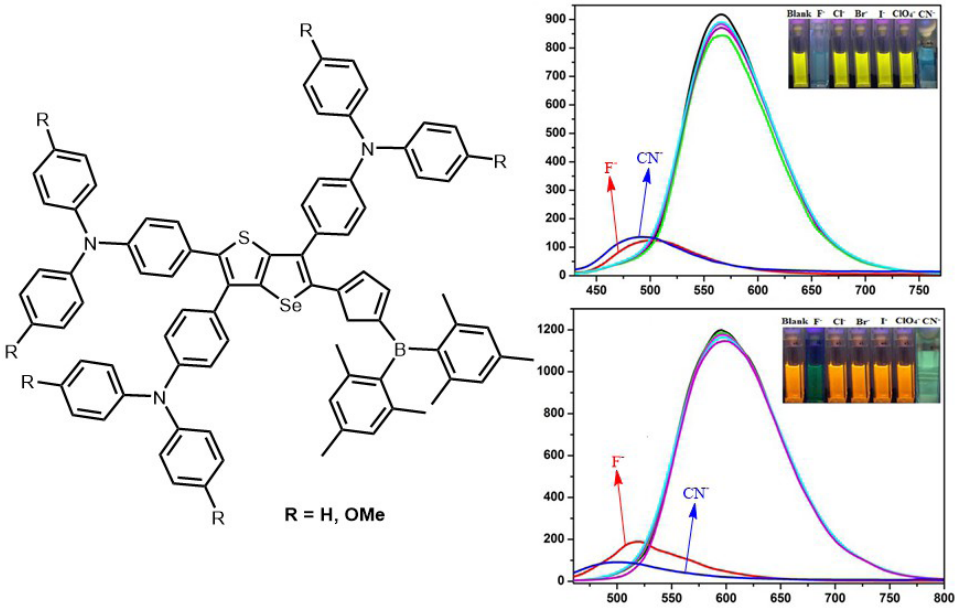

Figure 9. *Selenophenothiophene-cored triphenylamine analogues and their fluorogenic responses towards fluoride and cyanide anions.*

With the purpose of cation detection, Halay (2021) reported a novel triazine-cored ligand having a picolylamine group as the receptor, along with a fluorescent aminophenyl benzothiazole moiety (Figure 10). Photophysical experiments revealed that the fluorescent sensor candidate had the feature of AIE phenomenon with exhibited emission enhancement by polarity increment. In the recognition studies carried out using the DMSO:H2O mixture with the most appropriate polarity degree; highly selective and sensitive turn-on response was determined for Zn^{2+} cation over several potential interferant metal ions and the detection limit was found to be 0.011 μM.

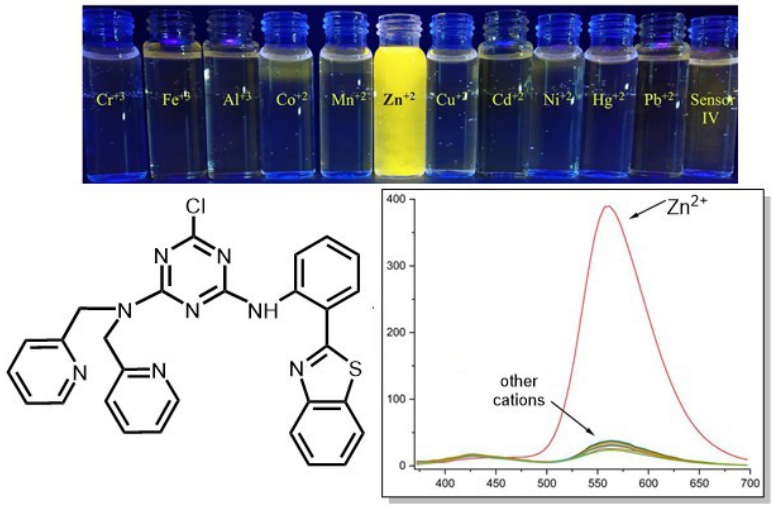

Figure 10. *A triazine-cored AIE sensor designed for Zn^{2+} detection.*

Orrego-Hernandez et al. (2016) developed a turn-on fluoroionophore in order to recognize alkaline earth metal Mg^{2+} without the interference of remaining metal ions in the same group II of the periodic table. They reported a Schiff base compound as s sensor candidate consisting of pyridylhydrazine and hydroxycoumarin moieties (Figure 11). Recognition studies with various metals, including alkali and transition metals revealed that Mg^{2+} ion selectively binds to the sensor compound with good binding ability. Besides transition metal ions have a strong interference on the selectivity of this sensor towards Mg^{2+}, it has been stated that Mg^{2+} recognition can be performed with high sensitivity without interference from similar metals found in alkali/alkaline earth groups such as sodium, potassium and calcium along with a low detection limit, 105 nM.

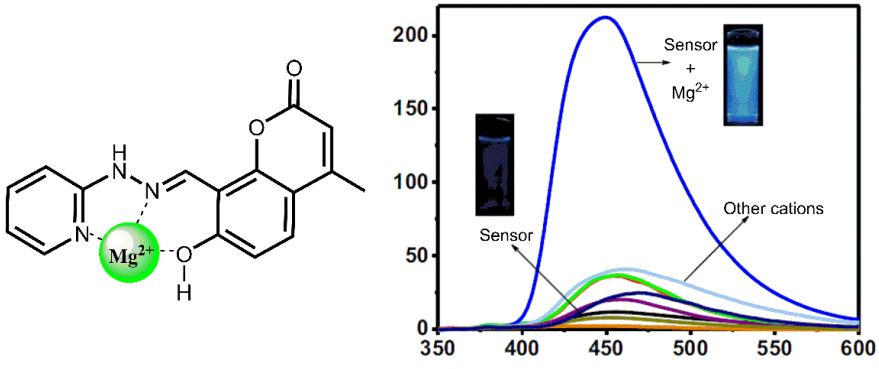

Figure 11. *A turn-on Schiff base sensor for Mg^{2+} ion derived from hydrazine/coumarin units.*

As a macrocyclic host molecule, Bozkurt et al. (2021) designed a fluoroionophore via linking approach using calix[4]arene macrocycle as receptor and aminophenylbenzothiazole fluorophore as reporter group (Figure 12). Over remaining such interferant anions like SO_4^{2-}, PO_4^{3-}, F^-, Cl^-, Br^-, I^-, ClO_3^-, and NO_3^-, this macrocyclic fluoroionophore was highly selective for CNO^- anion which was established through the standard method SM 4500-CN. Besides, calix[4]arene based sensor exhibit AIE feature that increased its sensitivity against CNO^- anion along with large Stokes' shift and colour change upon addition of CNO^-. Thus, based on the fact that cyanide ion turns into cyanate as a result of industrial waste treatment in many treatment plants, in the related study carried out by following the standard method SM 4500-CN, an important alternative for the determination of cyanide was constituted through the turn-on fluorometric determination of its oxidized form, cyanate, which is less harmful than cyanide.

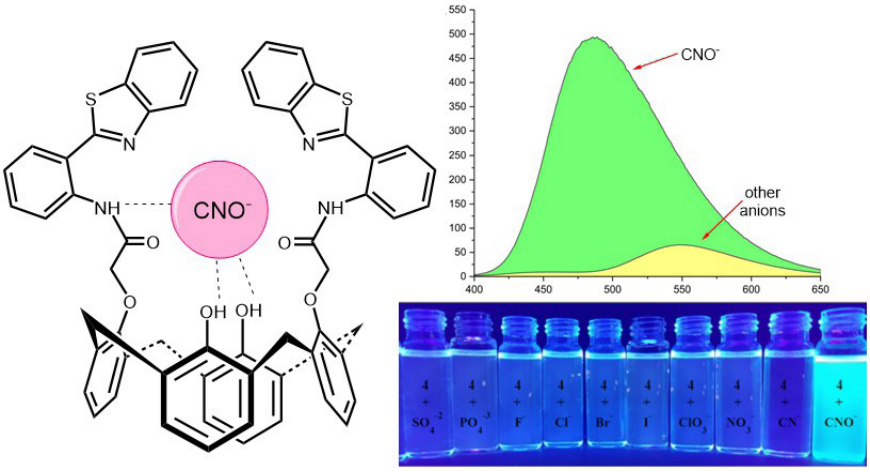

Figure 12. *Benzothiazole-armed calix[4]arene macrocycle as a turn-on cyanate sensor.*

Concluding Remarks

Luminescent materials stand a pivotal role in human daily life as light-emitting substances, as those have had a wide range of usage area such as security, astronomy, national defence and numerous optics. Moreover, and perhaps most importantly, when combined with appropriate molecular groups, those materials have been at the forefront by the works of applied sciences worldwide with their function as sensor materials in many areas that may affect human health. Hereby, synthesized multifunctional scaffolds have been used for dynamically monitoring/recognizing target metal

ions/small molecules/biomacromolecules and cellular microenvironments along with drug screening and disease diagnosis. Besides the fluorescence spectroscopy has been used as an extremely important technique to find the function of relevant molecules, the fluorescent responses of these organic probes also gain importance. Consequently, in order to conceive fluorescent ion recognition phenomena, the combination of structurally complementary reactants like ion hosts and fluorophores should be considered. In this context, herein, the recent applications of fluorescent ionophores have been summarized in order to provide more detailed and comprehensive understanding of ion probes with specific fluorescence feature and to encourage much more scientists for making some contributions to the development of those kind of sensors.

Different kinds of luminescent materials based on derivatives of organic molecules were tried to be discussed from their synthesis, recognition capabilities along with their proper mechanisms. These conclusions obtained in line with relevant review work can give some remarkable guidance for organic molecular design, synthesis and its applications and motivate all scientists to contribute their efforts for this kind of sensor research.

However, as a whole, the study of fluorophores for fluorescence ion recognition studies is still in the developmental stage and much more work needs to be done in the context of further expanding of molecular library and enriching this field. The pursuit of more selective, durable, and cost-effective fluorescent probes holds the potential to redefine how we detect and interpret ionic interactions across disciplines. It is believed that as this field advances, its applications will continue to expand beyond conventional laboratory works with an increased demand on the design and synthesis of novel fluorescent sensors.

In conclusion, it should not be forgotten that; just as walking and chewing gum simultaneously defies its perceived complexity, the evolution of fluorescence-based detection is making what once seemed intricate remarkably intuitive and bringing sophisticated ion recognition methods closer to effortless routine application.

References

Torres-Ocampo, A. P., Palmer, A. E. (2023). Genetically encoded fluorescent sensors for metals in biology. *Current Opinion in Chemical Biology*, *74*, Article 102284. https://doi.org/10.1016/j.cbpa.2023.102284

Kumari, N., Singh, S., Baral, M., Kanungo, B. K. (2023). Schiff bases: A versatile fluorescence probe in sensing cations. *Journal of Fluorescence*, *33*(3), 859–893. https://doi.org/10.1007/s10895-022-03135-6

Ahmed, N., Zareen, W., Yang, X., Shafiq, Z., Ye, Y. (2023). Development in fluorescent off–on probes based on Cu^{2+} promoted hydrolysis reaction of the picolinate moiety. *Journal of Fluorescence*, *33*(2), 401–411. https://doi.org/10.1007/s10895-022-03078-y

Nangare, S. N., Patil, A. G., Chandankar, S. M., Patil, P. O. (2023). Nanostructured metal-organic framework-based luminescent sensor for chemical sensing: Current challenges and future prospects. *Journal of Nanostructure in Chemistry*, *13*(2), 197–242. https://doi.org/10.1007/s40097-022-00479-0

Fang, Y., Deng, Y., Dehaen, W. (2020). Tailoring pillararene-based receptors for specific metal ion binding: From recognition to supramolecular assembly. *Coordination Chemistry Reviews*, *415*, Article 213313. https://doi.org/10.1016/j.ccr.2020.213313

Zheng, X., Cheng, W., Ji, C., Zhang, J., Yin, M. (2020). Detection of metal ions in biological systems: A review. *Reviews in Analytical Chemistry*, *39*(1), 231–246. https://doi.org/10.1515/revac-2020-0118

Zhong, X., Li, Z., Shi, R., Yan, L., Zhu, Y., Li, H. (2022). Schiff base-modified nanomaterials for ion detection: A review. *ACS Applied Nano Materials*, *5*(10), 13998–14020. https://doi.org/10.1021/acsanm.2c03477

Gupta, A., Rotake, D., Darji, A. (2024). Sensing lead ions in water: A comprehensive review on strategies and sensor materials. *Analytical Sciences*, *40*(6), 997–1021. https://doi.org/10.1007/s44211-024-00547-1

Langari, M. M., Antxustegi, M. M., Labidi, J. (2022). Nanocellulose-based sensing platforms for heavy metal ions detection: A comprehensive review. *Chemosphere*, *302*, Article 134823. https://doi.org/10.1016/j.chemosphere.2022.134823

Czarnik, A. W. (1993). Supramolecular chemistry, fluorescence, and sensing. In A. W. Czarnik (Ed.), *Fluorescent chemosensors for ion and molecule recognition* (pp. 1–9). American Chemical Society. https://doi.org/10.1021/bk-1993-0538.ch001

Wu, D., Sedgwick, A. C., Gunnlaugsson, T., Akkaya, E. U., Yoon, J., James, T. D. (2017). Fluorescent chemosensors: The past, present and future. *Chemical Society Reviews*, *46*(23), 7105–7123. https://doi.org/10.1039/c7cs00240h

Fan, Y., Wu, Y., Hou, J., Wang, P., Peng, X., Ge, G. (2023). Coumarin-based near-infrared fluorogenic probes: Recent advances, challenges and fu-

ture perspectives. *Coordination Chemistry Reviews*, *480*, Article 215020. https://doi.org/10.1016/j.ccr.2023.215020

Mukherjee, I. (2022). *Unexpected fluorescent behavior of maleimide based zwitterionic molecule: Aggregation induced emission*. ChemRxiv. https://doi.org/10.26434/chemrxiv-2022-7nns6

Verdejo, B., Inclan, M., Clares M. P., Bonastre-Sabater, I., Ruiz-Gasent, M., Garcia-Espana, E. (2022). Fluorescent chemosensors based on polyamine ligands: A review. *Chemosensors*, *10*(1), Article 1. https://doi.org/10.3390/chemosensors10010001

Kamel, R. M., El-Sakka, S. S., Abbas, M. M. A., Soliman, M. H. A. (2024). Eco-friendly fluorescent sensor for sensitive and selective detection of Zn^{2+} and Fe^{3+} ions: Applications in human hair samples. *Journal of Fluorescence*. https://doi.org/10.1007/s10895-024-03798-3

Senthil, J., Acharyulu, N. P. S., Krishnaveni, M., Mahalle, P. R., Thakur, S., Nakkella, A. K. (2024). Chemical sensors for environmental and medical diagnostics. *African Journal of Biological Sciences*, *6*(10), 6351–6368. https://doi.org/10.48047/AFJBS.6.10.2024.6351-6368

Fakayode, S. O., Lisse, C., Medawala, W., Brady, P. N., Bwambok, D. K., Anum, D., Alonge, T., Taylor, M. E., Baker, G. A., Mehari, T. F., Rodriguze, J. D., Elzey, B., Siraj, N., Macchi, S., Le, T., Forson, M., Bashiru, M., Narcisse, V. E. F., Grant, C. (2024). Fluorescent chemical sensors: Applications in analytical, environmental, forensic, pharmaceutical, biological, and biomedical sample measurement, and clinical diagnosis. *Applied Spectroscopy Reviews*, *59*(1), 1–89. https://doi.org/10.1080/05704928.2023.2177666

Fang, X., Zheng, Y., Duan, Y., Liu, Y., Zhong, W. (2019). Recent advances in design of fluorescence-based assays for high-throughput screening. *Analytical Chemistry*, *91*(1), 482–504. https://doi.org/10.1021/acs.analchem.8b05303

Wu, X., Barner-Kowollik, C. (2023). Fluorescence-readout as a powerful macromolecular characterisation tool. *Chemical Science*, *14*(45), 12815–12849. https://doi.org/ 10.1039/d3sc04052f

Singh, G., George, N., Singh, R., Singh G., Sushma, Kaur, G., Singh, H., Singh, J. (2023). Ion recognition by 1,2,3-triazole moieties synthesized via “click chemistry”. *Applied Organometallic Chemistry*, *37*(1), 1–62. https://doi.org/10.1002/aoc.6897

Yang, Y., Gao, F., Wang, Y., Li, H., Zhang, J., Zhiewi, S., Jiang, Y. (2022). Fluorescent organic small molecule probes for bioimaging and detection applications. *Molecules*, *27*(23), Article 8421. https://doi.org/10.3390/molecules27238421

Bin Darwish, N., Kurdi, A., Alshihri, S., Tabbakh, T. (2023). Organic heterocyclic-based colorimetric and fluorimetric chemosensors for the detection of different analytes: a review (from 2015 to 2022). *Materials Today Chemistry*, *27*, Article 101347. https://doi.org/10.1016/j.mtchem.2022.101347

Basheer, S. M., Rasin, P., Manakkadan, V., Palakkeezhillam, V. N. V., Sreekanth, A. (2023). Recent advancements in Schiff base fluorescence chemosensors for the detection of heavy metal ions. In T. Akitsu (Ed.), *Schiff base in organic, inorganic and physical chemistry*. IntechOpen. https://doi.org/10.5772/intechopen.109022

Park, S.-H., Kwon, N., Lee, J.-H., Yoon, J., Shin, I. (2020). Synthetic ratiometric fluorescent probes for detection of ions. *Chemical Society Reviews*, *49*(1), 143–179. https://doi.org/10.1039/c9cs00243j

Formica, M., Fusi, V., Giorgi, L., Micheloni, M. (2012). New fluorescent chemosensors for metal ions in solution. *Coordination Chemistry Reviews*, *256*(1-2), 170–192. https://doi.org/10.1016/j.ccr.2011.09.010

Suzuki, S., Sasaki, S., Sairi, A. S., Iwai, R., Tang, B. Z., Konishi, G.-I. (2020). Principles of aggregation-induced emission: design of deactivation pathways for advanced AIEgens and applications. *Angewandte Chemie-International Edition*, *59*(25), 9856–9867. https://doi.org/10.1002/anie.202000940

Pawar, S., Fegade, U., Bhardwaj, V. K., Singh, N., Bendre, R., Kuwar, A. (2015). 2-((E)-(2-aminophenylimino)methyl)-6-isopropyl-3-methylphenol based fluorescent receptor for dual Ni^{2+} and Cu^{2+} recognition: Nanomolar detection. *Polyhedron*, *87*, 79–85. http://dx.doi.org/10.1016/j.poly.2014.10.034

Xie, P., Zhu, Y., Huang, X., Gao, G., Wei, F., Guo, F., Jiang, S., Wang, C. (2019). A novel probe based on rhodamine 101 spirolactam and 2-(2′-hydroxy-5′-methylphenyl)benzothiazole moieties for three-in-one detection of paramagnetic Cu^{2+}, Co^{2+} and Ni^{2+}. *Spectrochimica Acta Part A: Molecular and Biomolecular Spectroscopy*, *222*, Article 117171. https://doi.org/10.1016/j.saa.2019.117171

Reddy, T. S., Moon, H., Choi, M.-S. (2021). Turn-on fluorescent naphthalimide-benzothiazole probe for cyanide detection and its two-mode aggregation-induced emission behavior. *Spectrochimica Acta Part A: Molecular and Biomolecular Spectroscopy*, *252*, Article 119535. https://doi.org/10.1016/j.saa.2021.119535

Gu, Y.-Q., Shen, W.-Y., Zhou, Y., Chen, S.-F., Mi, Y., Long, B.-F., Young, D. J., Hu, F.-L. (2019). A pyrazolopyrimidine based fluorescent probe for the detection of Cu^{2+} and Ni^{2+} and its application in living cells. *Spectrochimica Acta Part A: Molecular and Biomolecular Spectroscopy*, *209*, 141–149. https://doi.org/10.1016/j.saa.2018.10.030

Yang, X., Jin, L., Chen, Y., Zhong, X., Jiang, Y., Dai, Z. (2021). A novel aggregation induced emission probe based on coumarin scaffold for imaging hypochlorite in cells and zebrafish. *Journal of Photochemistry and Photobiology, A: Chemistry*, *419*, Article 113464. https://doi.org/10.1016/j.jphotochem.2021.113464

Kang, Z., Zhang, Z., Zhang, Y., Chen, S., Wang, J., Yuan, M.-S. (2022). Di-(2-picolyl)amine functionalized tetraphenylethylene as multifunctional che-

mosensor. *Analytica Chimica Acta*, *1196*, Article 339543. https://doi.org/10.1016/j.aca.2022.339543

Turkoglu, G., Ozturk, T. (2022). Fluorescent molecules with alternating triarylamine-substituted selenophenothiophene and triarylborane: Synthesis, photophysical properties and anion sensing studies. *Dalton Transactions*, *51*(7), 2715–2725. https://doi.org/10.1039/d1dt03681e

Halay, E. (2021). Cation sensing by a novel triazine-cored intermediate as a fluorescent chemosensor incorporating benzothiazole fluorophore. *Research on Chemical Intermediates*, *47*(10), 4281–4295. https://doi.org/10.1007/s11164-021-04534-3

Orrego-Hernandez, J., Nunez-Dallos, N., Portilla, J. (2016). Recognition of Mg^{2+} by a new fluorescent "turn-on" chemosensor based on pyridyl-hydrazono-coumarin. *Talanta*, *152*, 432–437. http://dx.doi.org/10.1016/j.talanta.2016.02.020

Bozkurt, S., Halay, E., Durmaz, M., Topkafa, M., Ceylan, Ö. (2021). A novel turn-on fluorometric "reporter-spacer-receptor" chemosensor based on calix[4]arene scaffold for detection of cyanate anion. *Journal of Heterocyclic Chemistry*, *58*(5), 1079–1088. https://doi.org/10.1002/jhet.4238

CHAPTER 2

EMERGING TRENDS IN POLYMER BASED BIOHYBRIDE MATERIALS

Gülce TAŞKOR ÖNEL[1]

1 Assoc. Prof. Gülce TAŞKOR ÖNEL, Erzincan Binali Yıldırım University, Faculty of Pharmacy, Dept. of Analytical Chemistry, ORCID: 0000-0002-9375-2329, gulce.onel@erzincan.edu.tr, gulcetaskor@gmail.com

INTRODUCTION

Polymer-based biohybrid materials derived from natural and synthetic sources are promising materials in the field of life sciences. These materials combine the biocompatibility and biodegradability of natural polymers with the durability and processability of synthetic polymers, enabling the process of making new materials with superior properties. In addition, polymeric biohybrid materials can also be advanced by coherence living cells and non-living materials to impart biomimetic functions to materials by promoting cell proliferation and improving cell functions. In this chapter on the structural design and structure-function relationships of biohydride materials, the author presents some promising strategies of polymeric biohydride materials to address the current challenges in the biomedical area, thanks to their superior biocompatibility and functional properties.

The main classes of synthetic polymers are carbon backbone polymers with hydrolysable functionalities such as esters, amides, urethanes and anhydrides. Natural polymers can be classified as proteins, carbohydrates and nucleic acids, which are produced by living organisms and can be found in nature. (Vroman & Tighzert, 2009) Polylactic acid(PLA) used in sutures, orthopaedic implants and drug delivery systems; polyglycolic acid (PGA) used in sutures; polyglycolic acid (PGA) used in drug delivery systems and tissue engineering; polycaprolactone (PCL) used in tissue engineering and drug delivery systems; poly(lactic-*co*-glycolic acid) (PLGA) commonly used in drug delivery systems and tissue engineering, polyurethanes used in heart valves, catheters and medical devices, polydimethylsiloxane (PDMS) used in soft tissue implants and microfluidic devices, polyacrylamide (PAM) used in wound dressings and lenses are synthetic biopolymers approved by the European Medicines Agency (EMA) and the US Food and Drug Administration (FDA). (Osorno et al., 2021) Examples of natural biopolymers include cellulose, which is found in plant cell walls; starch, which is used to store energy in plants; lignin, which gives plant cell walls their stiffness; collagen, keratin, silk which are formed by linking amino acids; chitin, which is found in the exoskeleton of insects and shellfish; polysaccharides, which are formed by linking sugar molecules produced by bacteria and fungi; and DNA and RNA, which carry genetic information, are formed by linking nucleotides and play a role in protein synthesis. (Sun et al., 2022)

BIOINSPIRED POLYMERIC MATERIALS

Developed through multidisciplinary studies, smart bio-inspired hybrid polymer materials have been commonly used in areas such as drug delivery, tissue engineering, biosensing and wearable medical tools. (Omi-

dian, Wilson, & Babanejad, 2023; Wegst, Bai, Saiz, Tomsia, & Ritchie, 2015; Yao, Wu, Liu, & Hua, 2024) Schlaad et al. reported that poly(2-oxazolines), known as pseudopeptides or bio-inspired polymers, could be synthesized by cationic ring opening polymerization and polymer modification techniques (click chemistry) and their solubility varies with the chemistry of the side chain, allowing the design of smart materials that can be adapted according to what is required for biomedical applications. The solubility temperature of poly(2-isopropyl-2-oxazoline) is close to human body temperature, and this excellent property makes it an ideal polymer for biomedical applications. A unique property of poly(2-isopropyl-2-oxazoline) is its ability to self-assemble into hierarchic colloidal particles via directional crystal growth from dilute hot aqueous solution, which is particularly exemplary of its bio-inspiring behavior. Although this process has not yet been fully elucidated, it appears to be highly compatible towards functional segments and chromatographic phases, suggesting that they are ideal materials for producing new composite materials (biosynthetic and organic-inorganic) with a hierarchic structure such as synthetic bone or tissue. It is reported that research in this direction is continuing. (Schlaad et al., 2010)

Gaharwar et al. discussed the insights and techniques needed to design new materials that mimic the complexity of natural textures and highlight key technological innovations that promise to advance the field. In one of the research studies in this review, composite bioadhesive microgels made from maleimide-functionalised polyethylene glycol network composites modelled by co-blending silicate nanoparticles and ionically cross-linked gelatin were prepared by a concerted design of microfabrication in combination with ionic gelation reaction and Michael addition chemistry. Clinically relevant anchorage-dependent cervical cancer cells were encapsulated and suspended leukemia cells as cell culture models for these composite microgel constructs and showed positive results in improved cell distribution, increased viability and metabolic activity compared to control gels. Composite bioadhesive hydrogels provide an important setting to study the independent effects of adhesive ligand density and physical stiffness on cell survival and function. The researchers noted that such cell-proliferation-enhancing microenvironments provide a more efficient cell culture environment that could be used to study cell survival and behaviour, without the need for harsh chemicals and UV cross-linking conditions. They also envision these biomaterials as promising building blocks for the fabrication of three-dimensional tissue constructs, cell delivery systems and tools for high throughput screening of new drugs. (Patel et al., 2014)

Beck-Broichsitter et al. showed that colloidal polymeric nanoparticles made of poly(lactide) coated with bio-inspired poly(2-methacryloyloxyethyl phosphorylcholine) (PMPC) caused a considerable loss of function of surfactant protein B (& C) from lung surfactant. They reported that phosphorylcholine-based poly(methacrylate) layer (i.e. PMPC) coated nanoparticles performed better than those coated with PEG and emphasised that it is important to consider biomimetic coatings during the design of nanoparticles to improve the biophysical functionality of the lung surfactant and for the therapy of lung diseases. (Beck-Broichsitter & Bohr, 2019)

In the review study by Zhao et al., the design templates of nature-inspired nanocrystalline cellulose (CNC) based materials, which mainly include mussels, mother-of-pearl and various plant species, were examined. (Zhao et al., 2023) Describing one of these templates, the study investigated novel stimulus-responsive, biomimetic, mechanically integrable nanocomposites that differentiate their mechanical properties when exposed to the action of water and form a water-activated shape memory. These materials were prepared by adding rigid cotton cellulose nanowhiskers (CNWs) to a rubbery polyurethane (PU) matrix. The films were then produced by compression moulding. When exposed to water, materials with CNW content above the filtration limit showed a slight swelling behaviour. The mechanically adaptive behaviour and high elasticity of wet materials are the basis for a shape memory effect using water as a stimulant. Polarised Raman spectroscopy revealed that CNWs exhibit a significant degree of uniaxial orientation in a transient manner, created by the stretching and drying of nanocomposites swollen with water. (Mendez et al., 2011)

BIOHYBRIDE PARTICLES

Compared to conventional biomaterials, biohybrid particles have significant advantages over traditional biomaterials, such as improved cellular compatibility, simpler and easier in vivo applicability, and the ability to achieve effective shaping/compatibility with material structures over time. To review a few notable examples from the literature; Liebscher et al. reported the synthesis and characterisation of magnetic core-shell nanoparticles (NPs) by surface-initiated polymerisation. NPs consist of a magnetic core and a polypyrol (PPy) shell with an azido function. NPs have several important applications in the fields of nanotechnology and nanomedicine,

as they can be manipulated by an external magnetic field and functionalised on their surface. In this study, the synthesis of superparamagnetic core-shell NPs with azido function PPy using the miniemulsion technique is reported for the first time. The new NPs are attractive for biomedical applications because PPy is biocompatible, the shell can be easily functionalised by the Cu-catalysed click reaction, and the material exhibits superparamagnetic behaviour. (Karsten, Nan, Turcu, & Liebscher, 2012)

Lahann and colleagues have reported the first study of a new micro-particulate biohybrid material containing anisotropic polymeric particles with spatially controllable kinship to human endothelial cells(HUVECs). These anisotropic polymeric particles are composed of two distinct sections with different functions, and this functional bipolarity is achieved by selective surface modification for the creation of polymer particles with two biologically distinct hemispheres: one showing high binding affinity for human endothelial cells and the other exhibiting actually cell_binding_ resistant behavior. Simultaneous electrohydrodynamic co-jetting of two different poly(acrylamide/poly(acrylic acid) copolymer (PAAm-co-AA) solutions was used to synthesise two-chamber particles. Such novel biomaterials were reported to be equally important for medical and biotechnological applications, including medical imaging, regenerative medicine and the design of new storage devices, actuators or energy gathering. (Yoshida et al., 2009)

In the review by Wang et al., research on physical and chemical ways to functionalise the algal surface with various reactive materials to the production of advanced bio-hybrid microalgae robots is presented. Representative practices of such algae-driven microparticle robots, including imaging, drug release and water decontamination, are highlighted. The distinct benefits of these active bio-hybrid robots are highlighted, along with their challenges and prospects. (Zhang et al., 2024) In a study highlighted in this review, Sitti et al. presented a new bio-hybrid swimmer design for cargo delivery. The use of natural swimmers as delivery vehicles offers an alternative strategy for delivering therapeutics to locations within the body that are difficult to reach with conventional delivery methods. Their design consists of 1 μm magnetic polystyrene particles (PS) functionalized with polyelectrolyte (PE) attached to an algae cell. The algae cells retain their natural motility and phototactic abilities, while the magnetic PS particles enable orientation and loading of therapeutics by an external magnetic field. Algae swimmers have been characterised in a variety of physiologically relevant provisions, including 3D swimming motility, cell culture media, human tubular fluid, blood and plasma. In addition, algae swimmers have been shown to be cytocompatible when co-cultured with cancerous and healthy cells. Finally, fluorescent isothiocyanate-dextran molecules were

efficiently delivered to mammalian cells using algae swimmers as an active cargo delivery display. The swimmer design described herein offers a novel bio-hybrid swimmer particle design with enhanced biocompatibility and mobility for targeted delivery applications in medicine. (Yasa, Erkoc, Alapan, & Sitti, 2018)

NANOBIOHYBRIDES

In Igor Nabiev's research, nanobio hybrid materials produced by conjugation of entraped molecules with excitonic (semiconductor) or plasmonic (metal) nanocrystals or microcures encoded with fluorescent semiconductor nanocrystals of distinct colours have reported a system aimed at the development of next-generation highly efficient diagnostic systems. A new generation of nanoprobes containing quantum dots (QDs) has been developed through the use of optically encoded nanocrystals. Quantum dots play an important role in medical diagnostic systems because of their high sensitivity and stability. The biocompatible properties of nanocrystals make them ideal for biomedical applications. These highly permeable nanoprobes can work effectively even in thick tissue. In particular, these probes are optimised for use in early cancer detection with high sensitivity, and the use of nanocrystals to label various biomolecules could revolutionise immunohistochemical analysis. (Nabiev, 2015)

Lee and co-authors published a review paper on the enhancement of a rapid and ultrasensitive detection system for miscellaneous pathogenic viral agents such as MERS-CoV, SARS-CoV, Dengue virus, Zika virus and especially avian influenza virus (AIV), which are highly infectious and create health, social and economic problems. This review discusses the feasibility of biosensors using nanobio hybrid materials for AIV, focusing on electrochemical, electrical, surface plasmon resonance and fluorescence-based detection methods. (Lee et al., 2018) In selected research from this review, Alocilja et al. developed a biosensor using surface plasmon resonance with electrically active magnetic (EAM) (polyaniline-coated AgNPs) nanoparticles. In studies on influenza A virus (FLUAV), EAM nanoparticles have experimentally demonstrated specific binding properties between haemagglutinin (HA) specificity and sialic acid, which plays a decisive role between human and animal infections. While this biosensor has an important application potential for the rapid and efficient detection of viruses, it is also reported to be of great importance in terms of biosafety measures. (Kamikawa et al., 2012)

REGENERATIVE MEDICINE APPLICATIONS

Polymers play a role in tissue scaffold design as key materials in the field of tissue engineering. When biopolymers act as biomaterials, they may be mimic of the extracellular matrix (ECM) of cells, enhance the biological behavior of cells in vitro and in vivo and affirm cellular behaviors. Since tissue engineering, cell growth and new tissue formation have advantages and disadvantages of synthetic, natural and hybrid polymer types alone, various materials can be used together and in composite form to develop physicochemical and biological properties. Important articles are reviewed below:

Guo et al. presented an approach that mimics the engineering of 3D cardiac anisotropy, which plays a crucial role in the construction of heart tissue. By developing 3D hybrid scaffolds composed of conductive nanofiber strands poly(caprolactone) (PCL), polyaniline (PANI), silk fibroin (SF), and carbon nanotubes (CNTs) (NFYs-NETs) arrayed in a hydrogel shell, the researchers were able to mimic natural texture of heart tissue and control cellular orientation. NFYs-NET constructs were used to provide orientation and maturation on cardiac muscle cells. The results obtained showed that these hybrid scaffolds enhanced the maturation of heart muscle cells (CMs) and were able to control cellular orientation in a 3D environment individually. Co-culturing of cardiac muscle cells with endothelial cells enhances vascularisation and promotes long-term cardiac tissue survival. The developed hybrid scaffolds have great potential for cardiac tissue engineering applications. (Wu, Wang, Guo, & Ma, 2017)

Depending on the target tissue, biopolymers can be designed to fulfil a range of specific functions. (Zarrintaj et al., 2023) Messina et al. presented a detailed study on the hydrodynamic and crowding differentiation of aqueous gelatin- hydroxyapatite hybrid systems. The aim is to increase knowledge about the biomimicry of collagen mineralisation and how it may be manipulated to prepare collagen-derived frameworks with specific morphological properties. Density measurements and viscosity determinations of the solution, together with spectroscopic techniques, revealed a progressive protein chain association that varied according to hydroxyapatite nanorods quantity. The effect of additives added to gelatin on the morphology of gelatin scaffolds has also been examined. Transverse and longitudinal profiles were obtained from the produced scaffolds and analysed using an optical microscope. It has been established that the porosity and geometry of the gelatin clusters may be readily modified through the modulation of the gelatin/HAp ratio in the solution employed as a pattern. (Sartuqui, D' Elía, Gravina, & Messina, 2015)

CELL THERAPY

Surface modification techniques are important to enhance vital functions by loading biomolecules into polymer-based biohybrid materials. Wang et al. demonstrated a simple and cost-effective way to modify porous poly(lactic-co-glycolic acid) (PLGA) microspheres with poly-L-lysine (PLL) to encourage cell growth on the microspheres. PLGA microspheres show multiple applications in the zone of tissue engineering because of their good biocompatibility, biodegradability and special shape. PLGA-PLL microspheres have been shown to be more suitable for MG63 cell attachment and proliferation due to increased initial cell binding amounts and improved cell matrix interactions. This novel modification procedure of porous PLGA microspheres has been proposed as a way to efficiently repair tissue defects at a reduced risk and cost level. (Yuan, Shi, Gan, & Wang, 2018)

Qian et al. designed an injectable thermo-sensitive hydrogel to provide spinal stability and fuse the bone matrix in the treatment of spinal disease. In this design, the hydrophobicity of collagen/nanohydroxyapatite (n-HA) / recombinant human BMP-2 @ Poly(ε-caprolactone)-PEG-poly(ε-caprolactone) copolymer (PCEC) / poly(ethylene glycol)-poly(ε-caprolactone)-poly(ethylene glycol) copolymer (PECE) hydrogels was improved with the use of poly(D, L-lactide) (PDLLA) electrospun nanofibre membrane to form a barrier between soft tissue and hydrogels. The system exhibited biocompatibility, preventing the escape of factors to ensure that they are retained in the necessary sites of osteogenesis, and the results showed an excellent effect on spinal fusion, they reported. (Qu et al., 2018)

In their research report, Krebsbach et al. sought to investigate the hypothesis that extracellular pH differences effect on gene expression of collagen, synthesis of collagen and alkaline phosphatase activity in bone marrow stromal cells (BMSCs). The impact of pH on cellular function is of particular significance in the related of tissue engineering, given that the fabrication of biocompatible polymers capable of establishing a local acidic microenvironment on biodegradation, the proliferation and differentiation of osteoblasts and the formation of mineralised tissue are dependent on the regulation of the pH value. Moreover, in the context of long-term organ culture on PLGA, it has been demonstrated that there is a gradual acidification of the culture medium up to pH 4.1, which has been shown to lead to a decrease in glycolysis, mineral content, and collagen synthesis. (Kohn, Sarmadi, Helman, & Krebsbach, 2002)

BIOMIMETIC MATERIALS

In the review by Patel et al., who also addressed the potential aspects in the improving of aerogel-based biomimetic scaffolds, it was stated that aerogels are lightweight and highly porous materials with great potential in biomedical research because of their unique properties, such as high surface area, tunable porosity and biocompatibility. Aerogel scaffolds have been shown to possess the capacity to function in a three-dimensional capacity as templates for the proliferation of cells, as well as for the promotion of wound healing, tissue regeneration and tissue repair. In addition, it has been reported that aerogel-based scaffolds, with their large surface area and porosity, are highly amenable to development in controlled drug delivery systems and enable effective loading and release of therapeutic agents into and out of the system. (Jeong, Patel, & Patel, 2024)

You and colleagues have developed biomimetic nanofibrous tissue scaffolds by combining natural silk protein nanofibrils and glycosaminoglycan hyaluronic acid (HA). The addition of hyaluronic acid functionality to the system has significantly increased the bioactivity and hydrophilicity of silk nanofibrils. Silk nanofibrils can be packaged on nanofibrous aerogel scaffolds at maximum scale in low density and designed shapes. The most striking point from this research is that hyaluronic acid silk nanofibrous aerogel scaffolds have been reported to have ultra high porosity, inherent bioactivity and structural stability in aqueous media. Silk nanofibrils scaffolds containing 10.0% hyaluronic acid were able to maintain their monolithic shape in protease/hyaluronidase solution for 3 weeks and longer. It has been demonstrated that silk nanofibrous scaffolds exhibit remarkable properties, which has led to their recognition as a biomaterial that not only replicates the composition of the ECM, but also its hierarchical structure. The result is a favourable microenvironment for cell adhesion and proliferation. The potential of this structurally and functionally biomimetic system as a promising tissue engineering biomaterial is highlighted in a review of the collective findings. (Li et al., 2024)

Li et al. investigated the concept of biomimetic nanofibrillation for high-strength structures mimicking spider silk. By copying the silk spinning principles of spiders, they strategically utilised the progressive integration of spatial shearing and high-pressure shearing to create silk-mimicking hierarchies in two phase biodegradable structures, namely Poly(lactic acid) (PLA) / Poly(butylene succinate) (PBS) blends. The incorporation of nanofibrils provides an exceptional combination of ductility, strength and toughness for nanofibrillar polymer composite materials. In particular, nanofibrils are reported to consist of aligned nanocrystals with a size of 1-6 nm and a concentration of ~20%. The proposed spider spinning mimicry strategy offered biomimetic function integration that cannot be achieved

by current approaches, encouraging materials scientists to pursue high-performance yet lightweight silk biopolymer mimics. (Xie et al., 2016)

BIOSENSORS

The integration of biopolymers into sensors is developing with the increasing demand for sensitive, selective and environmentally friendly detection strategies in life sciences. Doong and colleagues have reported their notes on the production of an unlabeled impedimetric immunosensor based on N,S-graphene quantum dots@Au-polyaniline nanowires for substance analysis of carcinoembryonic antigen. N,S-graphene quantum dots@Au-polyaniline nanowires were first synthesized by an easy hydrothermal pyrolysis process followed by interfacial polymerization techniques. At a later stage, 2-9 nm N,S-GQDs were successfully adapted on 30-50 nm Au-PANI nanowires with Au-thiol coupling by defining them as bifunctional probes to increase the electrochemical activity and at the same time make the anti_CEA stable. N,S-GQDs@Au-PANI nanowires have been identified as optimal conductive materials for accelerating electron transfer. Following the addition of carcinoembryonic antigen, the formation of carcinoembryonic antigen antibody antigen bioconjugates has been demonstrated to significantly enhance charge transfer resistance. This provides a label-free immunoassay and highly stable landing for the impedimetric detection of carcinoembryonic antigen. The label-free immunosensor exhibited a wide linear range from 0.5 to 1000 ng mL^{-1} with a low detection limit of 0.01 ng mL-1. The N,S-graphene quantum dots@Au-polyaniline-based immunosensor also shows high selectivity and stability over other cancer markers and amino acids. Furthermore, this promising platform is prosperously applied for the detection of carcinoembryonic antigen in human serum samples with an excellent recovery of (96.0±2.6)-(103±3.8)%. These results demonstrate the effectiveness of a newly developed high-throughput and label-free impedimetric immunosensor for the detection of carcinoembryonic antigen using N,S-graphene quantum dots@Au-polyaniline nanowires as biosensing probes, which may pave the way for the production of a high-performance and robust impedimetric immunosensor to determine cancer markers in the early stage of diagnosing and treating cancer. (Ganganboina & Doong, 2019)

Zhang and his colleagues have designed a disposable electrochemical immunosensor in their study. In this design, the principle of immobilization of a chitosan membrane modified with colloidal gold nanoparticles (AgNPs) on the indium-tin oxide (ITO) electrode surface of the antigen was considered for carcinoembryonic antigen (CEA). The structure characterization studies of the different membranes prepared by electrochemical methods and scanning electron microscopy were completed. Following a

highly competitive immunoassay procedure, the immobilized antigen of the immunosensor was incubated with an antibody labeled horseradish peroxidase (HRP) and a sample carcinoembryonic antigen, and the immunoconjugate accumulated in the immunosensor was detected by an o-phenylenediamine-H_2O_2-HRP electrochemical analysis. Under the most favorable experimental conditions, the electrocatalytic current decreased in direct proportion to the competitive mechanism. During the carcinoembryonic antigen analysis, the detection limit of 1.0 ng/ml was determined in the linear range of 2.0 to 20 ng/ml. The carcinoembryonic antigen immunosensor designed with this research is not only economical but also has good reproducibility and stability for mass production thanks to the cheap indium-tin oxide electrode obtained from industrial mass production. (Lin, Qu, & Zhang, 2007)

CONCLUSION AND FUTURE OUTLOOK

As a result, polymer-based bio-hybrid materials, derived from natural and synthetic sources, are emerging as promising materials in the field of life sciences. These materials enable the development of new materials with superior properties by combining the biocompatibility and biodegradability of natural polymers with the durability and processability of synthetic polymers. In addition, polymeric bio-hybrid materials can also be developed to provide biomimetic functions to materials by promoting cell proliferation and improving cell functions through the integration of living cells and non-living materials. In this chapter on structural design and structure-function relationships of bio-hybrid materials, the author presents some promising strategies of polymeric bio-hybrid materials to overcome the current challenges in the biomedical field, thanks to their superior biocompatibility and functional properties. In next-generation hybrid therapeutic systems, polymer-based biohybrid materials are also emerging in the role of enhancing bioavailability. Given the pace of research into polymer-based biohybrid materials, it is inevitable that bioinspired polymers, biohybrid particles, nanobiohybrids, regenerative medicine applications, next-generation cell therapy systems and biomimetic materials are set to become more effective and more widely used over the next decade.

REFERENCES

Beck-Broichsitter, M., & Bohr, A. (2019). Bioinspired polymer nanoparticles omit biophysical interactions with natural lung surfactant. *Nanotoxicology, 13*(7), 964-976. doi:10.1080/17435390.2019.1621400

Ganganboina, A. B., & Doong, R. A. (2019). Graphene Quantum Dots Decorated Gold-Polyaniline Nanowire for Impedimetric Detection of Carcinoembryonic Antigen. *Sci Rep, 9*(1), 7214. doi:10.1038/s41598-019-43740-3

Jeong, Y., Patel, R., & Patel, M. (2024). Biopolymer-Based Biomimetic Aerogel for Biomedical Applications. *Biomimetics, 9*(7). doi:10.3390/biomimetics9070397

Kamikawa, T. L., Mikolajczyk, M. G., Kennedy, M., Zhong, L., Zhang, P., Setterington, E. B., . . . Alocilja, E. C. (2012). Pandemic Influenza Detection by Electrically Active Magnetic Nanoparticles and Surface Plasmon Resonance. *IEEE Trans Nanotechnol, 11*(1), 88-96. doi:10.1109/tnano.2011.2157936

Karsten, S., Nan, A., Turcu, R., & Liebscher, J. (2012). A new access to polypyrrole-based functionalized magnetic core-shell nanoparticles. *Journal of Polymer Science Part A: Polymer Chemistry, 50*(19), 3986-3995. doi:https://doi.org/10.1002/pola.26193

Kohn, D. H., Sarmadi, M., Helman, J. I., & Krebsbach, P. H. (2002). Effects of pH on human bone marrow stromal cells in vitro: Implications for tissue engineering of bone. *Journal of Biomedical Materials Research, 60*(2), 292-299. doi:https://doi.org/10.1002/jbm.10050

Lee, T., Ahn, J.-H., Park, S. Y., Kim, G.-H., Kim, J., Kim, T.-H., . . . Lee, M.-H. (2018). Recent Advances in AIV Biosensors Composed of Nanobio Hybrid Material. *Micromachines, 9*(12). doi:10.3390/mi9120651

Li, X., Gao, Z., Zhou, S., Zhu, L., Zhang, Q., Wang, S., & You, R. (2024). Engineering biomimetic scaffolds by combining silk protein nanofibrils and hyaluronic acid. *International Journal of Biological Macromolecules, 257*, 128762. doi:https://doi.org/10.1016/j.ijbiomac.2023.128762

Lin, J., Qu, W., & Zhang, S. (2007). Electrochemical Immunosensor for Carcinoembryonic Antigen Based on Antigen Immobilization in Gold Nanoparticles Modified Chitosan Membrane. *Analytical Sciences, 23*(9), 1059-1063. doi:10.2116/analsci.23.1059

Mendez, J., Annamalai, P. K., Eichhorn, S. J., Rusli, R., Rowan, S. J., Foster, E. J., & Weder, C. (2011). Bioinspired Mechanically Adaptive Polymer Nanocomposites with Water-Activated Shape-Memory Effect. *Macromolecules, 44*(17), 6827-6835. doi:10.1021/ma201502k

Nabiev, I. (2015). Nano-bio Hybrid Materials for a New Generation of High-throughput Diagnostic Systems. *Physics Procedia, 73*, 95-99. doi:https://doi.org/10.1016/j.phpro.2015.09.127

Omidian, H., Wilson, R. L., & Babanejad, N. (2023). Bioinspired Polymers: Transformative Applications in Biomedicine and Regenerative Medicine. *Life, 13*(8). doi:10.3390/life13081673

Osorno, L. L., Brandley, A. N., Maldonado, D. E., Yiantsos, A., Mosley, R. J., & Byrne, M. E. (2021). Review of Contemporary Self-Assembled Systems for the Controlled Delivery of Therapeutics in Medicine. *Nanomaterials, 11*(2). doi:10.3390/nano11020278

Patel, R. G., Purwada, A., Cerchietti, L., Inghirami, G., Melnick, A., Gaharwar, A. K., & Singh, A. (2014). Microscale Bioadhesive Hydrogel Arrays for Cell Engineering Applications. *Cellular and Molecular Bioengineering, 7*(3), 394-408. doi:10.1007/s12195-014-0353-8

Qu, Y., Wang, B., Chu, B., Liu, C., Rong, X., Chen, H., . . . Qian, Z. (2018). Injectable and Thermosensitive Hydrogel and PDLLA Electrospun Nanofiber Membrane Composites for Guided Spinal Fusion. *ACS Applied Materials & Interfaces, 10*(5), 4462-4470. doi:10.1021/acsami.7b17020

Sartuqui, J., D' Elía, N., Gravina, A. N., & Messina, P. V. (2015). Analyzing the hydrodynamic and crowding evolution of aqueous hydroxyapatite-gelatin networks: Digging deeper into bone scaffold design variables. *Biopolymers, 103*(7), 393-405. doi:https://doi.org/10.1002/bip.22645

Schlaad, H., Diehl, C., Gress, A., Meyer, M., Demirel, A. L., Nur, Y., & Bertin, A. (2010). Poly(2-oxazoline)s as Smart Bioinspired Polymers. *Macromolecular Rapid Communications, 31*(6), 511-525. doi:https://doi.org/10.1002/marc.200900683

Sun, Y., Bai, Y., Yang, W., Bu, K., Tanveer, S. K., & Hai, J. (2022). Global Trends in Natural Biopolymers in the 21st Century: A Scientometric Review. *10*. doi:10.3389/fchem.2022.915648

Vroman, I., & Tighzert, L. (2009). Biodegradable Polymers. *Materials, 2*(2), 307-344. doi:10.3390/ma2020307

Wegst, U. G. K., Bai, H., Saiz, E., Tomsia, A. P., & Ritchie, R. O. (2015). Bioinspired structural materials. *Nature Materials, 14*(1), 23-36. doi:10.1038/nmat4089

Wu, Y., Wang, L., Guo, B., & Ma, P. X. (2017). Interwoven Aligned Conductive Nanofiber Yarn/Hydrogel Composite Scaffolds for Engineered 3D Cardiac Anisotropy. *ACS Nano, 11*(6), 5646-5659. doi:10.1021/acsnano.7b01062

Xie, L., Xu, H., Li, L.-B., Hsiao, B. S., Zhong, G.-J., & Li, Z.-M. (2016). Biomimetic Nanofibrillation in Two-Component Biopolymer Blends with Structural Analogs to Spider Silk. *Sci Rep, 6*(1), 34572. doi:10.1038/srep34572

Yao, N., Wu, J., Liu, G., & Hua, Z. (2024). Bioinspired and biomimetic nucleobase-containing polymers: the effect of selective multiple hydrogen bonds. *Chemical Science, 15*(45), 18698-18714. doi:10.1039/D4SC06720G

Yasa, O., Erkoc, P., Alapan, Y., & Sitti, M. (2018). Microalga-Powered Microswimmers toward Active Cargo Delivery. *Advanced Materials, 30*(45), 1804130. doi:https://doi.org/10.1002/adma.201804130

Yoshida, M., Roh, K.-H., Mandal, S., Bhaskar, S., Lim, D., Nandivada, H., . . . Lahann, J. (2009). Structurally Controlled Bio-hybrid Materials Based on Unidirectional Association of Anisotropic Microparticles with Human Endothelial Cells. *Advanced Materials, 21*(48), 4920-4925. doi:https://doi.org/10.1002/adma.200901971

Yuan, Y., Shi, X., Gan, Z., & Wang, F. (2018). Modification of porous PLGA microspheres by poly-l-lysine for use as tissue engineering scaffolds. *Colloids and Surfaces B: Biointerfaces, 161*, 162-168. doi:https://doi.org/10.1016/j.colsurfb.2017.10.044

Zarrintaj, P., Seidi, F., Youssefi Azarfam, M., Khodadadi Yazdi, M., Erfani, A., Barani, M., . . . Mozafari, M. (2023). Biopolymer-based composites for tissue engineering applications: A basis for future opportunities. *Composites Part B: Engineering, 258*, 110701. doi:https://doi.org/10.1016/j.compositesb.2023.110701

Zhang, F., Li, Z., Chen, C., Luan, H., Fang, R. H., Zhang, L., & Wang, J. (2024). Biohybrid Microalgae Robots: Design, Fabrication, Materials, and Applications. *Advanced Materials, 36*(3), 2303714. doi:https://doi.org/10.1002/adma.202303714

Zhao, X., Bhagia, S., Gomez-Maldonado, D., Tang, X., Wasti, S., Lu, S., . . . Ozcan, S. (2023). Bioinspired design toward nanocellulose-based materials. *Materials Today, 66*, 409-430. doi:https://doi.org/10.1016/j.mattod.2023.04.010

CHAPTER 3

MOLECULAR DOCKING ANALYSIS OF SYNTHESIZED NEW IMINE COMPOUND

Büşra KÖLEMENOĞLU[1]

Burçin TÜRKMENOĞLU[2]

Zülbiye KÖKBUDAK[3]

1 MSc, Department of Chemistry, Institute of Science, Erciyes University, Kayseri, Türkiye

ORCID ID: 0009-0000-8352-8270

2 Assoc. Prof. Dr., Department of Analytical Chemistry, Faculty of Pharmacy, Erzincan Binali Yıldırım University, Erzincan, Türkiye

ORCID ID: 0000-0002-5770-0847

3 Prof. Dr., Department of Chemistry, Faculty of Science, Erciyes University, Kayseri, Türkiye

*Corresponding Author: Email: zulbiye@erciyes.edu.tr

ORCID ID: 0000-0003-2413-9595

1. Introduction

Pyrimidines, which are heterocyclic aromatic organic compounds, contain two nitrogen atoms at positions **1** and **3** of the ring.. In recent years, pyrimidine derivatives have gained importance in new syntheses and biological activity research. Pyrimidine incorporated compounds have diverse applications in many fields of pharmaceutical, agricultural, and material sciences. They have pharmacological applications such as antifungal, anticonvulsant, antiviral, antitubercular, antineoplastic, anthelmintic, anticancer properties (Figure 1). Literature reports have shown that $–NH_2$ group, *p*-methoxyphenyl nucleus, Ar–Br group, *p*-dimethyl amino phenyl nucleus, *p*-chloro and *p*- nitrobenzylideneamino groups are effective on the biological activity of the pyrimidine ring. (Abu-Hashem, El-Shehry, & Badria, 2010; Amir, Javed, & Kumar, 2007; Basavaraja, Sreenivasa, & Jayachandran, 2005; Dea-Ayuela et al., 2009; Juby, Hudyma, Brown, Essery, & Partyka, 1979; Kappe, 1993; Kumar, Khan, Tekwani, Ponnan, & Rawat, 2015; Ram, Haque, & Guru, 1992; Smith & Kan, 1964)**.** Pyrimidine derivatives containing amino group (-NH2) can enter into reactions due to their functional group. These reactions are nucleophilic substitution, acylation, alkylation, reductive amination, cyclization reactions.

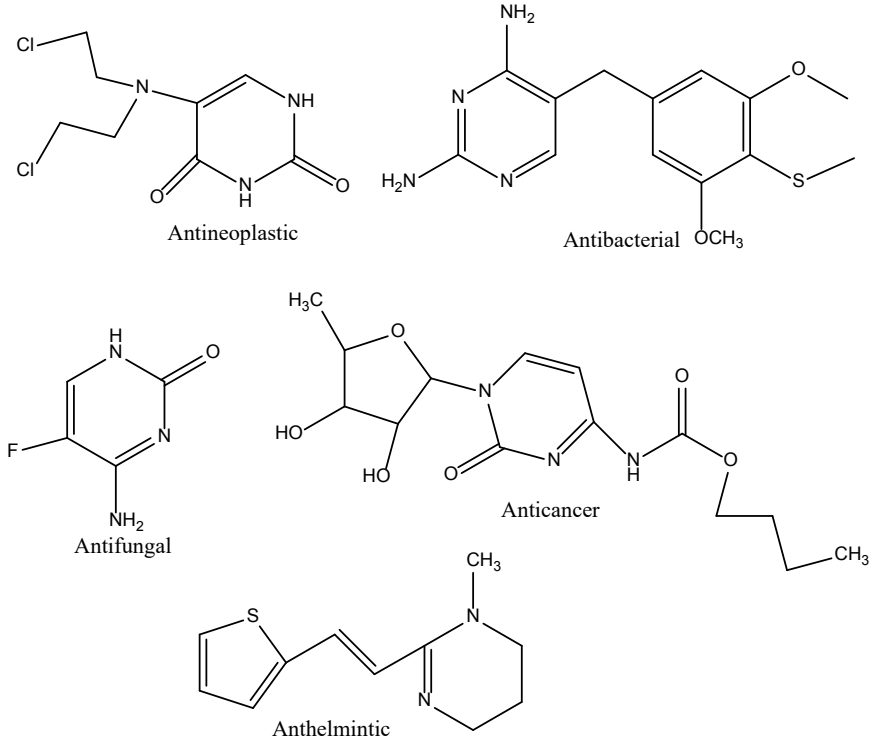

Figure 1. *Some of the bioactive molecules containing pyrimidine.*

Schiff bases (imines) are formed by condensing primary amines with the carbonyl groups and can also be represented by the general formula RCH = NŔ. The substituents can encompass aryl, alkyl, heteroaryl, or cycloalkyl groups (Dea-Ayuela et al., 2009). In recent years, biological, analytical and industrial applications of Schiff bases have gained great importance (Majumdar & Chattopadhyay, 2011). Biological properties of Schiff bases and metal complexes have been reported in such as, antibacterial, antifungal, anticancer, anticonvulsant, anti-HIV, antiprotozoal and herbicidal activities (Amer, El-Wakiel, & El-Ghamry, 2013; Bensaber et al., 2014; Güngör & Gürkan, 2014; Pontiki, Hadjipavlou-Litina, & Chaviara, 2008; Shanty et al., 2017).

Prompted by aforementioned facts, in the present work, we have planned to synthesize pyrimidine Schiff base of ***(Z)-1-((4-methoxynaphthalen-1-yl)methyleneamino)-5-(4-methylbenzoyl)-4-p-tolylpyrimidin-2(1H)-thione.*** For this reason, at first, via reaction of furan-2,3-dion and semicarbazon in benzene, amino pyrimidine (**K1**) as reagent was synthesized. And then, a new imine compound (**K2**) was synthesized by the reaction of 4-methoxy-1-naphthaldehyde and compound (**K1)** under reflux conditions (Scheme 2). Molecular structure of compound (**K2)** was characterized by ^{1}H-NMR, ^{13}C-NMR.

Aminopyrimidine compounds synthesized from these activities are among the basic compounds used in medicinal chemistry. Bioactive molecules containing pyrimidine have recently become attractive in drug design since they are used in medicinal chemistry. They are being investigated in both structure-based and ligand-based drug design methods due to their specified activity properties. In this study, their anticancer and Alzheimer's disease properties were investigated theoretically, namely by the molecular docking method.

2. Materials and Method

2.1. Experimental

All solvents and reagents used in synthesis were bought commercial companies like sigma-aldrich, merck, alfa easer and used without further purification. ^{1}H-NMR and ^{13}C-NMR spectra were recorded on a Bruker 400 MHz Ultra Shield instrument. Melting point of compound (**K2**) was determined by digital melting point apparatus (Electrothermal 9100).

2.2. Synthesis of Schiff Base

2.2.1. (Z)-1-((4-methoxynaphthalen-1-yl)methyleneamino)-5-(4-methylbenzoyl)-4-p-tolylpyrimidin-2(1H)-thione (K2)

1 mmol the starting compound (**K1**) and 1.5 mmol 4-methoxy-1-naphthaldehyde were taken in a reaction flask and 30 mL of ethyl alcohol was added as solvent and *p*-toluene sulfonic acid (PTSA) as catalyst. Then the mixture had been refluxed for 6 hours. The reaction was regularly controlled by TLC. The precipitated was filtered off and recrystallized by ethyl alcohol.The structure of (**K2**) was determined by using analytical and spectroscopic methods. Yield: (70%); m.p.: 201-202 ^{o}C; color: white. ^{1}H-NMR (400 MHz, DMSO-d_6) δ (ppm) = 9.30 (s, 1H), 9.19 (d, J = 8.5 Hz, 1H), 8.99 (s, 1H), 8.30 (d, J = 8.2 Hz, 1H), 8.10 (d, J = 6.8 Hz, 1H), 7.84 (d, J = 6.6 Hz, 2H), 7.74 (t, J = 7.6 Hz, 1H), 7.64 (t, J = 7.4 Hz, 1H), 7.46 (d, J = 6.6 Hz, 2H), 7.30 (d, J = 7.4 Hz, 2H), 7.20 (d, J = 7.0 Hz, 3H), 4.09 (s, 3H), 2.34 (s, 3H), 2.29 (s, 3H). ^{13}C NMR (101 MHz, DMSO-d_6) δ (ppm) = 191.63, 169.63, 159.66, 146.19, 145.07, 141.55, 135.23, 133.77, 132.16, 130.55, 130.41, 129.91, 129.88, 129.56, 129.41, 129.04, 126.96, 126.74, 125.95, 125.40, 124.74, 122.57, 120.54, 104.93, 56.76, 21.66, 21.40. Molecular Formula: $C_{31}H_{25}N_3O_2S$ and Formula Weight: (503.615 g/mol).

2.3. Molecular Docking

Schrödinger Maestro 14.1 program (Schrödinger Release 2024-3: Glide) was used in the theoretical investigation of the imine compound by molecular docking method. The molecular docking method is applied in three stages. First, the preparation of compound **K2** by LigPrep wizard, the second step is the determination and preparation of the target protein, and the third step is the interaction of the ligand and target *in silico.* The protocol specified in previous studies was applied in the molecular docking method (BozbeyMerde, Önel, Türkmenoğlu, Gürsoy, & Dilek, 2022; Merde et al., 2022; TÜRKMENOĞLU, 2022a, 2022b). The ligand was optimized with the LigPrep wizard. In the second stage, the crystal structures of the specified targets were obtained from the protein data bank. The water molecules in the target preparation environment were removed with the ProteinPrep wizard. In the last stage, the prepared **K2** ligand and the target were interacted *in silico* to determine the binding modes and binding parameter values.

3. Results and Discussion

3.1. Experimental

The compound (**K1)** was prepared from the furan-2,3-dione derivative using the method specified in the literature. A new Schiff base (**K2**) was synthesized by the condensation of compound (**K1**) with 4-methoxy-1-naphthaldehyde at 70% (Scheme 1). The compound was purified by recrystallization. Synthesis of Schiff bases are usually carried out by reactions of amines with carbonyl compounds by addition and subtraction. Schiff bases are stable at room temperature and are non-hygroscopic. The compounds are insoluble in water but are soluble in DMSO.

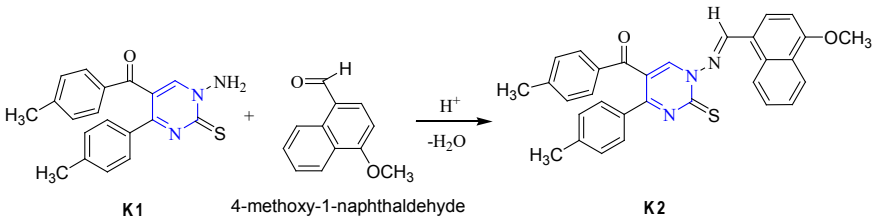

Scheme 1. *Synthesis scheme of compound (***K2***).*

In the ^{1}H NMR spectra of the imine derivatives, the striking peak belongs to the azomethine proton. In the ^{1}H NMR spectrum, the N=CH proton was resonated at δ 9.30 ppm. The proton signal for -CH in the pyrimidine ring for (**K2)** was detected singlet at δ 8.99 ppm. Aromatic protons were observed as multiplet between δ 8.30 and 7.20 ppm. Also, methoxy proton was observed at 4.09 ppm and methyl protons were determined at 2.34 and 2.29 ppm. In the ^{13}C NMR spectrum, benzoyl carbon's signal was observed at δ 191.63 ppm. The signals of CH_3O- group was observed at 56.76 ppm as singlet. Other carbons of the molecule were obtained between δ 169.63-21.40 ppm. The data obtained because of the analyses fully confirmed the structure of Schiff base.

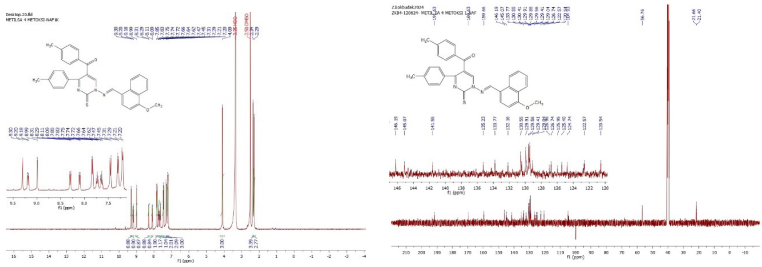

Scheme 2. *^{1}H NMR and ^{13}C NMR Spectrums of compound (***K2***).*

3.2. Molecular Docking

The interactions of compound **K2** obtained through the synthesis study with possible targets were analyzed computationally. Thus, the binding modes of compound **K2**, which was interacted in silico, were calculated. The current method supporting this is molecular docking. Three different targets were determined with molecular docking, one of the structure-based drug design methods, and **K2** was interacted with in order. While determining the targets, crystal structures related to anti-cancer and Alzheimer's disease were determined. In other words, compound **K2** was interacted with 1M17 (Stamos, Sliwkowski, & Eigenbrot, 2002), which is the Epidermal Growth Factor Receptor (EGFR), with 3ERT (Shiau et al., 1998), which is the crystal structure of the Estrogen Receptor (ER), and with 4EY7 (Cheung et al., 2012), which is the acetylcholinesterase enzyme (AChE). The binding values of the results of these interactions are presented in Table 1.most striking computational results are the *in silico* calculations performed against Alzheimer's disease.

Table 1. *Parameter values of the interactions of compound* **K2** *with 1M17, 3ERT and 4EY7 crystal structures via in silico approaches.*

PDB ID	Compound	Docking Score	Glide Gscore	Glide Energy	Glide Emodel
1M17	**Compound K2**	-3.525	-3.525	-46.133	-71.118
	Erlotinib	-9.469	-9.469	-55.987	-77.117
3ERT	**Compound K2**	-9.676	-9.676	-35.998	-16.979
	Tamoxifen	-11.300	-11.324	-54.896	-88.073
4EY7	**Compound K2**	-8.879	-8.879	-53.061	-84.262
	Tacrine	-7.234	-7.234	-33.526	-46.405

The binding parameter values of compound **K2** presented in Table 1 provide theoretical preliminary information. The binding parameter values presented are considered separately for both reference compounds and possible binding of **K2** for three different targets. Thus, it can be theoretically interpreted whether **K2**, which is compared with reference compounds in terms of binding modes, can be a drug candidate. The first target is the EGFR crystal structure that prevents the spread of cancer. While the docking score value of EGFR and **K2** is -3.525 kcal/mol, the docking score value of Erlotinib is -9.469 kcal/mol. This shows that there are differences in terms of binding parameter values. In addition, 2D and 3D diagrams of EGFR and **K2** are presented in Figure 2. In Figure 2, **K2** has a hydrogen bond with Cys773 and Met769 amino acid residues.

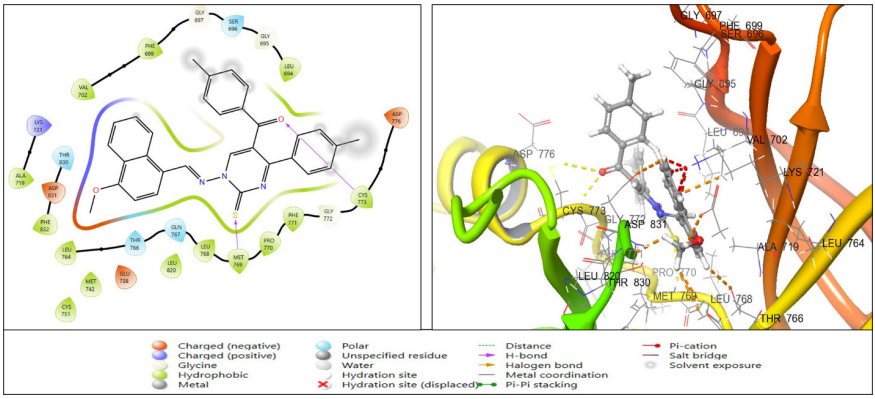

Figure 2. *Binding modes of compound* **K2** *with EGFR (PDB ID: 1M17).*

As in Table 1, the second target is 3ERT, the estrogen receptor. The crystal structure of 3ERT was interacted with both **K2** and Tamoxifen in silico. The docking score, Glide gscore, Glide energy and Glide emodel values are shown in Table 1 as the interaction results. The interactions of 3ERT and **K2** were compared with Tamoxifen. The docking score value of 3ERT and **K2** is -9.676 kcal/mol, while the docking score value of Tamoxifen is -11.300 kcal/mol. These values were calculated to be quite close to each other. It can be said that the **K2** compound is effective on the estrogen receptor according to the computational results. In addition, when the 2-dimensional and 3-dimensional interaction diagrams between **K2** and 3ERT are examined in Figure 3, it was determined that the compound was docked in the active binding site. In Figure 3, there is also a hydrogen bond with the Cys530 amino acid residue in the 2-dimensional interaction diagram.

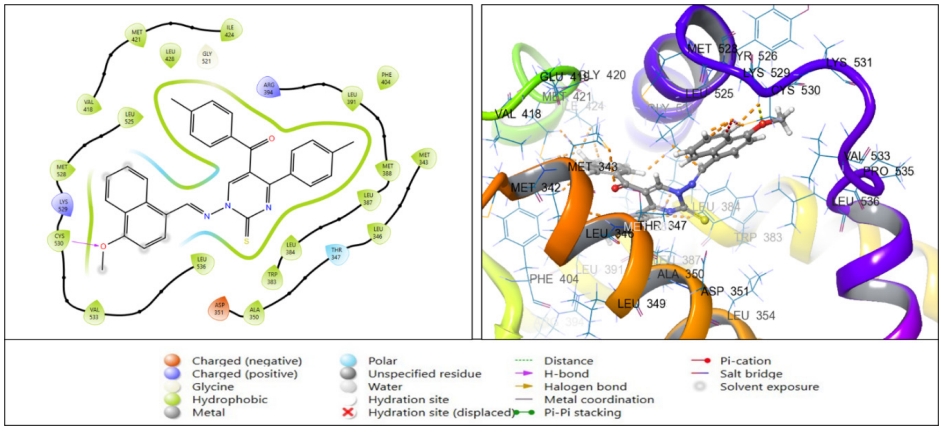

Figure 3. *Binding modes of compound* **K2** *with Estrogen Receptor (PDB ID: 3ERT).*

Both **K2** and Tacrine were interacted with the crystal structure of the last target, acetylcholinesterase enzyme, by molecular docking method in silico environment. It was determined according to Table 1 that after the target of estrogen receptor, acetylcholinesterase enzyme is also effective in binding angle. In Table 1, the interaction results of **K2** and 4EY7 crystal structure are docking score -8.879 kcal/mol, Glide model -84.262 kcal/mol, Glide energy -53.061 kcal/mol, respectively. When the values of reference compound Tacrine are examined, the docking score is -7.234 kcal/mol, which is a lower value. All of the interaction values with Tacrine and 4EY7 are calculated to be lower than **K2**.

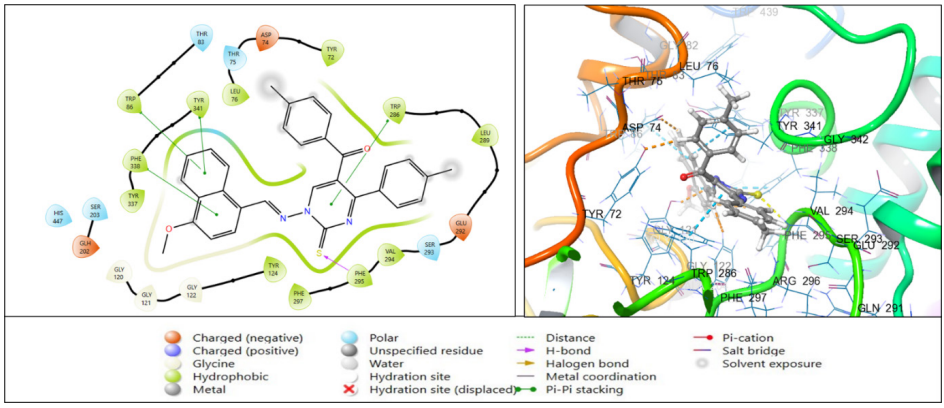

Figure 4. *Binding modes of compound* **K2** *with AChE (PDB ID: 4EY7).*

For all three targets, detailed in silico analysis of compound **K2** was performed. In addition, visualization and computational results of the interactions of this compound with estrogen receptor, EGFR and AChE were presented. The results of compound **K2** on both estrogen receptor and AChE among the three targets are remarkable. In addition, it was shown that **K2**, which is docked in the active pocket region of the crystal structure, interacts with the desired amino acid residues in the 2D interaction diagrams.

4. CONCLUSION

In this study, a new pyrimidin-2(1*H*)-thione derivative (**K2**) was prepared and examined with *in silico* approaches. The structure of the synthesized heterocyclic compound **K2** was determined experimentally. Synthesized **K2** was analyzed in silico in this study. Binding modes and binding parameter values were taken into consideration more during the analysis. Since a comparison values will always be more effective, Tacrine for AChE, Tamoxifen for ER and Erlotinib for EGFR were used as comparison compounds in the targets. These comparison compounds were

compared with **K2** for each target. The most remarkable result for the synthesized **K2** compound was determined to be in AChE and Estrogen receptor targets. Thus, computational results that can be a precursor to other studies were obtained.

References

Abu-Hashem, A. A., El-Shehry, M. F., & Badria, F. A.-E. (2010). Design and synthesis of novel thiophenecarbohydrazide, thienopyrazole and thienopyrimidine derivatives as antioxidant and antitumor agents. *Acta pharmaceutica, 60*(3), 311-323.

Amer, S., El-Wakiel, N., & El-Ghamry, H. (2013). Synthesis, spectral, antitumor and antimicrobial studies on Cu (II) complexes of purine and triazole Schiff base derivatives. *Journal of Molecular Structure, 1049*, 326-335.

Amir, M., Javed, S., & Kumar, H. (2007). Pyrimidine as Antiinflammatory Agent: A Review. *Indian journal of pharmaceutical sciences, 69*(3).

Basavaraja, H., Sreenivasa, G., & Jayachandran, E. (2005). Synthesis and biological activity of novel pyrimidino imidazolines. *Indian Journal of Heterocyclic Chemistry, 15*, 69.

Bensaber, S. M., Allafe, H., Ermeli, N. B., Mohamed, S. B., Zetrini, A. A., Alsabri, S. G., . . . Gbaj, A. M. (2014). Chemical synthesis, molecular modelling, and evaluation of anticancer activity of some pyrazol-3-one Schiff base derivatives. *Medicinal Chemistry Research, 23*, 5120-5134.

BozbeyMerde, İ., Önel, G. T., Türkmenoğlu, B., Gürsoy, Ş., & Dilek, E. (2022). (p-Chlorophenyl)-3 (2H) pyridazinone Derivatives: Synthesis, in Silico, and AChE/BChE Inhibitory Activity. *ChemistrySelect, 7*(38), e202202446.

Cheung, J., Rudolph, M. J., Burshteyn, F., Cassidy, M. S., Gary, E. N., Love, J., . . . Height, J. J. (2012). Structures of human acetylcholinesterase in complex with pharmacologically important ligands. *Journal of Medicinal Chemistry, 55*(22), 10282-10286.

Dea-Ayuela, M. A., Castillo, E., Gonzalez-Alvarez, M., Vega, C., Rolón, M., Bolás-Fernández, F., . . . González-Rosende, M. E. (2009). In vivo and in vitro anti-leishmanial activities of 4-nitro-N-pyrimidin-and N-pyrazin-2-ylbenzenesulfonamides, and N2-(4-nitrophenyl)-N1-propylglycinamide. *Bioorganic & medicinal chemistry, 17*(21), 7449-7456.

Güngör, Ö., & Gürkan, P. (2014). Synthesis and characterization of higher amino acid Schiff bases, as monosodium salts and neutral forms. Investigation of the intramolecular hydrogen bonding in all Schiff bases, antibacterial and antifungal activities of neutral forms. *Journal of Molecular Structure, 1074*, 62-70.

Juby, P. F., Hudyma, T. W., Brown, M., Essery, J. M., & Partyka, R. A. (1979). Antiallergy agents. 1. 1, 6-dihydro-6-oxo-2-phenylpyrimidine-5-carboxylic acids and esters. *Journal of Medicinal Chemistry, 22*(3), 263-269.

Kappe, C. O. (1993). 100 years of the Biginelli dihydropyrimidine synthesis. *Tetrahedron, 49*(32), 6937-6963.

Kumar, D., Khan, S. I., Tekwani, B. L., Ponnan, P., & Rawat, D. S. (2015). 4-Aminoquinoline-pyrimidine hybrids: synthesis, antimalarial activity, heme bin-

ding and docking studies. *European journal of medicinal chemistry, 89*, 490-502.

Majumdar, K. C., & Chattopadhyay, S. K. (2011). *Heterocycles in natural product synthesis*: John Wiley & Sons.

Merde, İ. B., Önel, G. T., Türkmenoğlu, B., Gürsoy, Ş., Dilek, E., Özçelik, A. B., & Uysal, M. (2022). Synthesis of (p-tolyl)-3 (2H) pyridazinone Derivatives as Novel Acetylcholinesterase Inhibitors. *ChemistrySelect, 7*(28), e202201606.

Pontiki, E., Hadjipavlou-Litina, D., & Chaviara, A. T. (2008). Evaluation of anti-inflammatory and antioxidant activities of copper (II) Schiff mono-base and copper (II) Schiff base coordination compounds of dien with heterocyclic aldehydes and 2-amino-5-methyl-thiazole. *Journal of Enzyme Inhibition and Medicinal Chemistry, 23*(6), 1011-1017.

Ram, V., Haque, N., & Guru, P. (1992). Chemotherapeutic agents. XXV: Synthesis and leishmanicidal activity of carbazolylpyrimidines. *European journal of medicinal chemistry, 27*(8), 851-855.

Schrödinger Release 2024-3: Glide, S., LLC, New York, NY, 2024.

Shanty, A. A., Philip, J. E., Sneha, E. J., Kurup, M. R. P., Balachandran, S., & Mohanan, P. V. (2017). Synthesis, characterization and biological studies of Schiff bases derived from heterocyclic moiety. *Bioorganic chemistry, 70*, 67-73.

Shiau, A. K., Barstad, D., Loria, P. M., Cheng, L., Kushner, P. J., Agard, D. A., & Greene, G. L. (1998). The structural basis of estrogen receptor/coactivator recognition and the antagonism of this interaction by tamoxifen. *Cell, 95*(7), 927-937.

Smith, P. A., & Kan, R. O. (1964). Cyclization of Isothiocyanates as a Route to Phthalic and Homophthalic Acid Derivatives1, 2. *The Journal of Organic Chemistry, 29*(8), 2261-2265.

Stamos, J., Sliwkowski, M. X., & Eigenbrot, C. (2002). Structure of the epidermal growth factor receptor kinase domain alone and in complex with a 4-anilinoquinazoline inhibitor. *Journal of Biological Chemistry, 277*(48), 46265-46272.

TÜRKMENOĞLU, B. (2022a). Investigation of Nirmatrelvir with Different Crystal Structures Effective on SARS-CoV-2 by In Silico Approaches. *Journal of the Institute of Science and Technology, 12*(3), 1615-1623.

Türkmenoğlu, B. (2022b). Investigation of novel compounds via in silico approaches of EGFR inhibitors as anticancer agents. *Journal of the Indian Chemical Society, 99*(8), 100601.

CHAPTER 4

INVESTIGATION OF NEW IMINE COMPOUND THROUGH IN VITRO AND SILICO APPROACHES

Burcu SOMTÜRK YILMAZ[1]

Burçin TÜRKMENOĞLU[2]

Zülbiye KÖKBUDAK[3]

1 Dr., Drug Application and Research Center, Erciyes University, 38280 Kayseri, Türkiye

ORCID ID: 0000-0002-2775-3083

2 Assoc. Prof. Dr., Department of Analytical Chemistry, Faculty of Pharmacy, Erzincan Binali Yıldırım University, Erzincan, Türkiye

ORCID ID: 0000-0002-5770-0847

3 Prof. Dr., Department of Chemistry, Faculty of Science, Erciyes University, Kayseri, Türkiye

*Corresponding Author: Email: zulbiye@erciyes.edu.tr

ORCID ID: 0000-0003-2413-9595

1. Introduction

As a significant class of heterocyclic compounds, pyrimidines occupy an outstanding status in medicinal and organic chemistry since they display a broad spectrum of biological activities such as anti-inflammatory and analgesic, antimicrobial, anti influenza, anti-cancer, against HSV-1 (herpes simplex virus type-1) and HAV (hepatitis-A virus) activities (Abu-Zaied, Elgemeie, & Mahmoud, 2021; Akkoc et al., 2023; KarataŞ, Burak, & Zulbiye, 2022; Khalifa, Al-Omar, Amr, Baiuomy, & Abdel-Rahman, 2015; Kökbudak, Akkoç, Karataş, Tüzün, & Aslan, 2022; Shaffer, Emerson, Murphy, Govindarajan, & Lemon, 1995; Zabihollahi et al., 2013) There are many commercially available pyrimidine-incorporated drugs on the market (**Figure 1**).

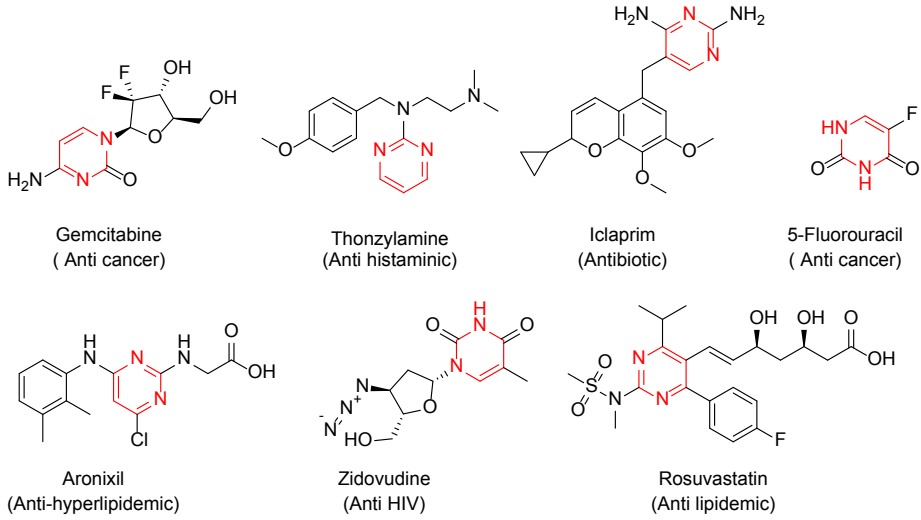

Figure 1. *Some pyrimidine group-bearing drugs at market*

Since its first discovery by Hugo Schiff in 1884, Schiff base, also called azomethine or imine, has been a remarkable group of biologically and industrially important compounds. They exhibit remarkable biological activities including antimicrobial, antiviral, antifungal, anti-inflammatory, anticancer, and antipyretic agents (Akkoc, Tüzün, Özalp, & Kökbudak, 2021; Murtaza et al., 2017).

Polar substituents incorporated Schiff bases process as more potent ligands corrosion inhibitors compared to unsubstituted ones. The polar groups enter the electron transfer mechanism using its unbonded electrons while Azomethine group interplay with the metal atom by using π-electron transfer mechanism (dπ-pπ bond). Transition metal complexes of imines

are also broadly employed as catalysts for many chemical reactions (Agrawal, Talati, Shah, Desai, & Shah, 2004; Gupta & Sutar, 2008).

Prompted by aforementioned facts, in the present work, we have planned to synthesize pyrimidine Schiff base of (*Z*)-(1-((4-Bromobenzylidene) amino)-2-thioxo-4-(*p*-tolyl)-1,2-dihydropyrimidin-5-yl)(*p*-tolyl)methanone (**B2**). For this reason, at first, via reaction of furan-2,3-dion and semicarbazon in benzene, amino pyrimidine (**B1**) as reagent was synthesized (Agrawal et al., 2004; Gupta & Sutar, 2008; Önal & Yıldırım, 2007). And then, a new imine compound **B2** was synthesized by the reaction of 4-bromobenzaldehyde and compound **B1** under reflux conditions (**Scheme 1**). Molecular structure of compound **B2** was characterized by various spectral techniques including FTIR, ^{1}H-NMR and ^{13}C-NMR.

Cancer is a very important public health problem. It also continues to exist as a life-threatening disease (Bray et al., 2018; Rolland, 2005). Cancer cases are increasing rapidly today. And it causes approximately 10 million deaths per year (Mattiuzzi & Lippi, 2019). Today, cancer research continues to progress rapidly in search of new drug candidates. New treatments such as immunotherapy and targeted therapies are being developed and tested in clinical trials. Therefore, researchers have made great progress in understanding the disease and finding new ways to treat cancer. However, it is thought that there is still much to learn about cancer treatment (Hassan, Moustafa, & Awad, 2017). Therefore, designing and synthesizing anti-cancer drug molecules with increased efficacy in order to treat cancer with minimum toxicity is among the first goals. In this context, it is thought that the synthesis of (Z)-(1-((4-bromobenzylidene)amino)-2-thioxo-4-(p-tolyl)-1,2-dihydropyrimidin-5-yl)(p-tolyl)methanone molecule can be carried out and it can be an anti-cancer drug molecule. Therefore, (Z)-(1-((4-bromobenzylidene)amino)-2-thioxo-4-(p-tolyl)-1,2-dihydropyrimidin-5-yl) (p-tolyl)methanone was synthesized and its anticancer activities were tested on A549 and MCF7 cell lines.

2. Materials and Method

2.1. Experimental

The reagents and solvents used in synthesis were purchased from different chemical companies. The purities of the compounds were routinely monitored using DC Alufolien Kieselgel 60 F254-Merck thin layer chromatography and Camag brand TLC lamp (254/366 nm). This study also used electrothermal 9100 brand digital melting point device, Shimadzu Model 8400 FT-IR spectrophotometer, Bruker brand 400 MHz (for ^{1}H NMR) and 100 MHz (for ^{13}C NMR) spectrophotometer. The starting

material **B1** has been prepared according to literature procedures (Önal & Yıldırım, 2007)**.** The synthesis steps are given in **Scheme 1.**

2.2. Synthesis of Schiff Base

2.2.1. (Z)-(1-((4-Bromobenzylidene)amino)-2-thioxo-4-(*p*-tolyl)-1,2-dihydropyrimidin-5-yl)(*p*-tolyl)methanone (B2)

Mixtures of compound **B1** (1 mmol) and 4-bromobenzaldehyde (1.5 mmol) in 30 mL of ethanol were refluxed in the presence of a catalytic amount of *p*-toluene sulfonic acid as catalyst for 8 h. The solvent was evaporated after this reaction time. Then, the residue was treated with dry diethyl ether and filtered. This Schiff base **B2** was purified with crystallization in ethyl alcohol. The structure of **B2** was determined by using analytical and spectroscopic methods. Yield: (65%); m.p.: 188-190 ^{o}C; color: yellow. ^{1}H NMR (400 MHz, DMSO-d_6) δ 8.93 (s, 2H), 7.84 (dt, J = 8.8, 4.8 Hz, 6H), 7.44 (d, J = 6.6 Hz, 2H), 7.30 (d, J = 7.0 Hz, 2H), 7.20 (d, J = 7.1 Hz, 2H), 2.35 (s, 3H), 2.29 (s, 3H). ^{13}C NMR (101 MHz, DMSO) δ 191.50, 168.84, 145.91, 145.12, 141.65, 134.13, 133.64, 132.74, 131.52, 131.48, 130.55, 129.92, 129.62, 129.56, 129.42, 129.36, 127.26, 120.52, 21.67, 21.41. FT-IR: 3053.2 (aromatic C-H), 2909.6 (aliphatic C-H), 1650.5 (C=O), 1593.1-1463.5 (C=N and C=C), 1254.1 (C=S), 761.2-744.9 cm^{-1} (pyrim.). Molecular Formula: $C_{26}H_{20}N_3OS$ and Formula Weight: 502.43.

2.3. Cytotoxicity assessment (MTT assay)

MTT ([3-(4,5-dimethylthiazol-2-yl)− 2,5 diphenyltrazolium bromide]) test was applied to determine the doses to be used in geno-toxicity studies of the synthesized **B2** molecule. For this purpose, the A549 cell was seeded at a density of 12 500 cells/well in a 96-well plate, while for MCF-7 cell it was seeded at a density of 5000 cells/well and incubated overnight.

The determination of the concentrations to be used in the MTT test by considering the biological activity studies, and the application was conducted by gradually decreasing the concentrations starting from the highest concentration (125 µg/mL). For this reason, after adding **B2** organic molecule (1.95–125µg/mL) synthesized to the culture medium, it was left to incubate for 24 h. The absorbance of the wells was measured using a microplate reader at a wavelength of 572 nm. The effect of **B2** molecule on the viability of A549 and MCF7 cells were evaluated as the percentage of cell viability (Somturk-Yilmaz, Altiparmak, Turkmenoglu, & Akkoc, 2024; Somturk-Yilmaz, Turkmenoglu, & Akkoc, 2024; Somturk Yilmaz, 2024; Yilmaz et al., 2024).

2.4. Statistical Analysis

All data were expressed as the mean values ± SD. Statistical analysis was performed by one-way ANOVA followed by Dunnett's multiple comparisons test using GraphPad Prism 8.0.2. $P < 0.05$ was considered as statistically significant.

2.5. Molecular Docking

Calculations were performed to support the in vitro results of compound **B2** via *in silico* approaches. These calculations were performed using the LigPrep, ProteinPrep, Glide docking interfaces of the Schrödinger Maestro 14.1 program (Schrödinger Release 2024-3: Glide). The procedure described in previous studies was applied (Merde, Onel, Turkmenoglu, Gursoy, & Dilek, 2022; Türkmenoğlu, 2022). The mechanism of the interactions between ligand and target was elucidated by molecular docking performed in three steps. In addition, the binding parameter values were also calculated.

3. Results and Discussion

3.1. Experimental

In this study, pyrimidine-2-thione derivative B**1** was used as a key starting material. The compound B**1** was prepared according to the literature method by a two-step process (Önal & Yıldırım, 2007). Reactions of **1** with aromatic aldehydes afforded the Schiff base derivatives **2-6** in satisfactory yields (60-76%) (see experimental section) (**Scheme 1**). The moderate yield of the reactions can be explained by the chemical behaviour of pyrimidine-2-thione **B1** towards the aromatic aldehydes (**Scheme 1**). Compound **B2** was obtained from the reaction of compound **B1** and 4-bromobenzaldehyde in 65% yield. In the FT IR spectrum of compound **B1**, the -NH_2 absorption bands are found to be at 3262 cm^{-1} (Önal & Yıldırım, 2007). The Shiff base formed over the NH_2 group, which lost protons of compound **B1**. The C=O and C=S absorption bands were observed at 1643 and 1221 cm^{-1}. The N=CH stretching vibrations were observed between 1593.1-1463.5 cm^{-1}. In ^{1}H NMR spectrum of compound **B2**: The signal of N=CH was observed at 8.93 ppm. The aromatic (CH) of **B2** were detected between 7.84-7.20 ppm. The signals of methyl protons in the structure of **B2** were detected at 2.35, 2.29 ppm as singlets. The carbons of -CH_3 groups were observed at 21.67, 21.41 ppm as singlets. The carbon atoms of **B2** were determined in the 191.50-120.52 ppm region. The results of

measurements were given in the experimental section. The general outline of the reaction studied is shown in **Scheme 1**.

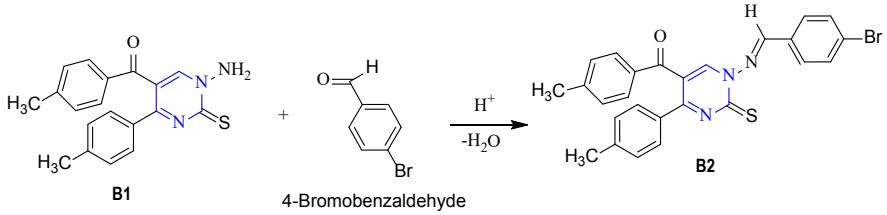

Scheme 1. *Synthesis of compound (***B2***).*

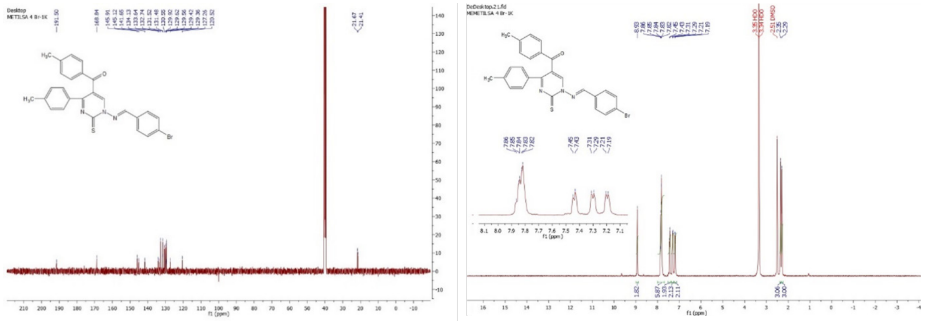

Scheme 2. *^{1}H NMR and ^{13}C NMR Spectra of compound (***B2***).*

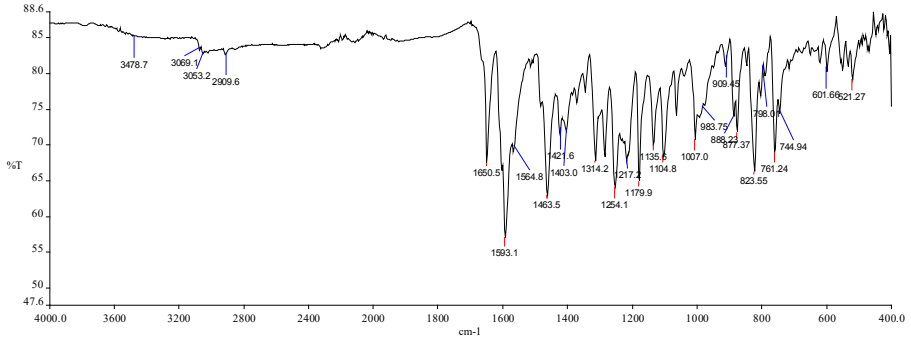

Scheme 3. *FT-IR Spectrum of compound (***B2***).*

3.2. Cytotoxicity assessment

The effect of compound **B2** on the viability of A549 and MCF7 cell lines is shown in Fig. 1. On A549 and MCF7 lines, seven different concentrations (1.95-3.9– 7.81–15.625–31.25–62.5–125 µg/mL) were applied. It was observed that the anticancer activity of the synthesized B2 organic molecule was quite effective in both the A549 cell line and MCF7 cell line.

When Figure 2 was examined, it was observed that the effectiveness of the synthesized **B2** organic molecule increased due to the increase in concentration. When the two graphs were examined, it was concluded that

the **B2** organic molecule was more effective on the MCF7 cell. The compound **B2** caused approximately 50% cell death in the A549 cell, while it caused 70% cell death in the MCF7 cell. According to the statistical data in Figure 2, when the comparison was made between the control group and **B2** organic molecule, ** $p < 0.01$, ***$p < 0.001$, ****p 0.0001. $P < 0.05$ was considered as statistically significant.

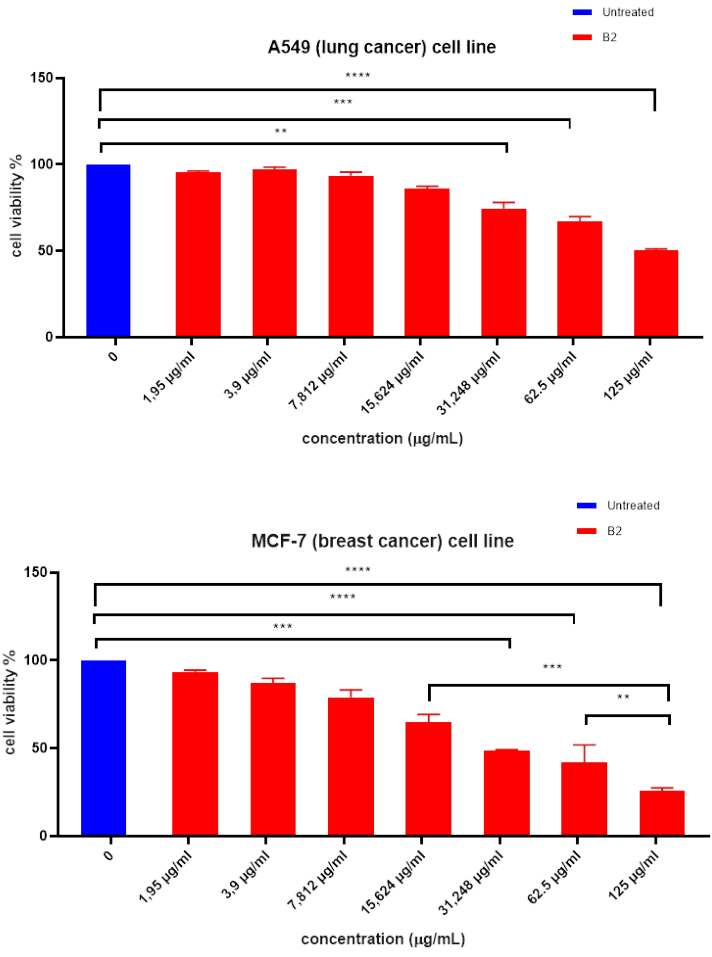

Figure 2. *Cytotoxicity of* **B2** *molecule on A549 and MCF7 cells lines, respectively. Data were presented as mean±SD. **p<0.01, ***p<0.001, ****p<0.0001*

3.3. Molecular Docking

Experimentally obtained by synthesis, compound **B2** was investigated in vitro as an anticancer. In addition to these studies, studies with molecular docking from in silico approaches were also performed. In short, it was presented that the experimentally obtained data also supported theoretically.

In molecular docking, two different targets were taken into consideration and interaction regions, and parameter values were calculated. As the first target, the crystal structure of Epidermal Growth Factor Receptor was obtained and downloaded from the protein data bank (https://www.rcsb.org/structure/1M17) (Stamos, Sliwkowski, & Eigenbrot, 2002). Then, the interaction of compound **B2** with the first target was provided. The binding parameter values of the interaction of compound **B2** with EGFR and the interaction amino acids in the active pocket region were presented. As the second target, when studies were applied on breast cancer in vitro, it was determined as an estrogen receptor. The relevant crystal structure of the estrogen receptor was also downloaded from the protein data bank (https://www.rcsb.org/structure/3ERT) and interacted with compound **B2** (Shiau et al., 1998).

Table 1. *Molecular docking results of compound* **B2**.

PDB ID	Compound	Docking Score	Glide Gscore	Glide Energy	Glide Emodel
1M17	**Compound B2**	-4.748	-4.748	-29.342	-55.611
	Erlotinib	-9.469	-9.469	-55.987	-77.117
3ERT	**Compound B2**	-5.117	-5.117	-41.932	-53.475
	Tamoxifen	-11.300	-11.324	-54.896	-88.073

The binding score values of **B2** interacting with EGFR, which was determined as the first target, are shown in Table 1. This binding value was compared with Erlotinib, the co-crystallized ligand of EGFR. In Table 1, the docking score value of compound B2 for EGFR is -4.748 kcal/mol, while the value of Erlotinib is -9.469 kcal/mol. This shows that compound B is not as strong as Erlotinib. The 2D and 3D interaction poses of compound B2 with the target are shown in Figure 3.

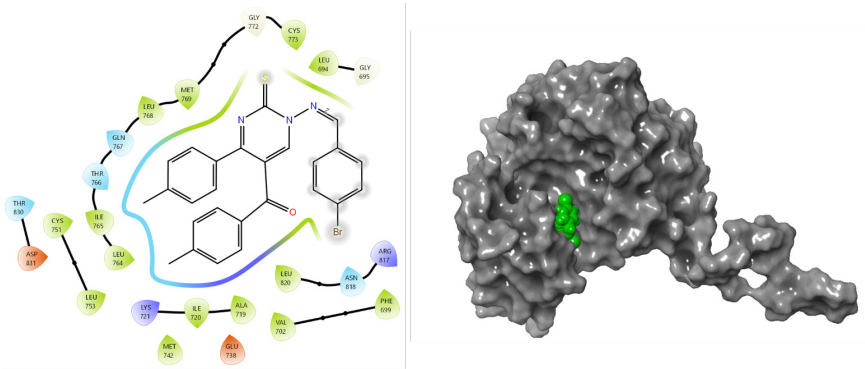

Figure 3. *Binding modes of compound* **B2** *with EGFR (PDB ID: 1M17).*

Figure 3 presents the 2D pose of **B2** interacting with EGFR and the 3D poses of the active binding site. It was determined that the compound fully occupies the active site of the target. The interaction results of compound **B2** with the 3ERT crystal structure for the second target, the estrogen receptor, are shown in Table 1.

Another target was determined as an estrogen receptor. The numerical results of the interaction of compound **B2** with the obtained crystal structure of this target are presented in Table 1. The crystal structure interacted with both **B2** and Tamoxifen. The interaction results of compound **B2** with the target of estrogen receptor in Table 1 are shown in Table 1. The docking score values of **B2** are -5.117 kcal/mol, while that of Tamoxifen is -11.300 kcal/mol.

When these values are compared, it is determined that Tamoxifen is theoretically better than compound **B2** and it is calculated that they are quite close to each other.

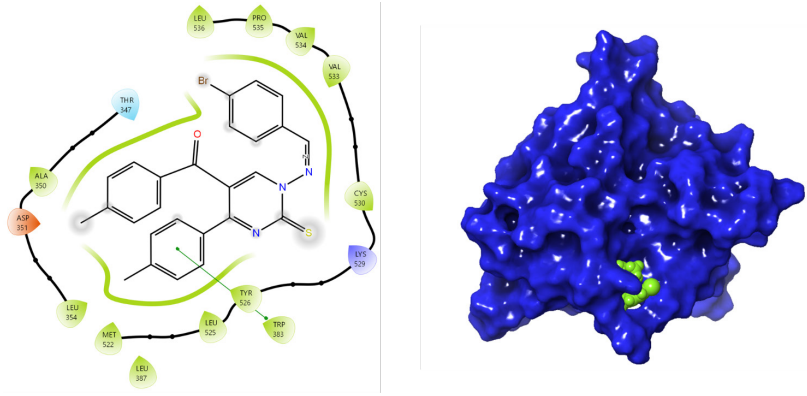

Figure 4. *Binding modes of compound* **B2** *with Estrogen Receptor (PDB ID: 3ERT).*

The 2D interaction diagram of the crystal structure of **B2** and estrogen receptor and the poses where it is docked in the 3D active pocket region are presented in Figure 4. The 2-dimensional interaction diagram of compound **B2**, which completely fits into the active pocket region of 3ERT, shows that there is a π-π stacking interaction with the phenyl ring and the Trp383 amino acid residue in Figure 4. It was also understood that compound **B2** fits into the active binding site determined in the crystal structure in Figure 4 from the correct side.

4. CONCLUSION

In this study, a new pyrimidin-2(1*H*)-thione derivative (**B2**) was prepared and examined with *in silico* approaches. The structure of the synthesized heterocyclic compound **B2** was determined experimentally. When Compound **B2** was analyzed separately on both cell lines, it was observed in vitro that it could be effective. For both targets, the interactions with compound **B2** in molecular docking were analyzed in terms of active binding. The results of the interactions with EGFR and estrogen receptor as anticancer agents were presented in silico. Thus, both in vitro and in silico methods were analyzed together.

References

Abu-Zaied, M. A., Elgemeie, G. H., & Mahmoud, N. M. (2021). Anti-covid-19 drug analogues: synthesis of novel pyrimidine thioglycosides as antiviral agents against SARS-COV-2 and avian influenza H5N1 viruses. *ACS Omega, 6*(26), 16890-16904.

Agrawal, Y. K., Talati, J. D., Shah, M. D., Desai, M. N., & Shah, N. K. (2004). Schiff bases of ethylenediamine as corrosion inhibitors of zinc in sulphuric acid. *Corrosion Science, 46*(3), 633-651.

Akkoc, S., Karatas, H., Muhammed, M. T., Kökbudak, Z., Ceylan, A., Almalki, F., . . . Ben Hadda, T. (2023). Drug design of new therapeutic agents: Molecular docking, molecular dynamics simulation, DFT and POM analyses of new Schiff base ligands and impact of substituents on bioactivity of their potential antifungal pharmacophore site. *Journal of Biomolecular Structure and Dynamics, 41*(14), 6695-6708.

Akkoc, S., Tüzün, B., Özalp, A., & Kökbudak, Z. (2021). Investigation of structural, electronical and in vitro cytotoxic activity properties of some heterocyclic compounds. *Journal of Molecular Structure, 1246*, 131127.

Bray, F., Ferlay, J., Soerjomataram, I., Siegel, R. L., Torre, L. A., & Jemal, A. (2018). Global cancer statistics 2018: GLOBOCAN estimates of incidence and mortality worldwide for 36 cancers in 185 countries. *CA: a cancer journal for clinicians, 68*(6), 394-424.

Gupta, K. C., & Sutar, A. K. (2008). Catalytic activities of Schiff base transition metal complexes. *Coordination Chemistry Reviews, 252*(12-14), 1420-1450.

Hassan, A. S., Moustafa, G. O., & Awad, H. M. (2017). Synthesis and in vitro anticancer activity of pyrazolo [1, 5-a] pyrimidines and pyrazolo [3, 4-d][1, 2, 3] triazines. *Synthetic Communications, 47*(21), 1963-1972.

KarataŞ, H., Burak, T., & Zulbiye, K. (2022). Could pyrimidine derivative be effective against Omicron of SARS-CoV-2? *Bratislava Medical Journal, 123*(7).

Khalifa, N. M., Al-Omar, M. A., Amr, A. E.-G. E., Baiuomy, A. R., & Abdel-Rahman, R. F. (2015). Synthesis and biological evaluation of some novel fused thiazolo [3, 2-a] pyrimidines as potential analgesic and anti-inflammatory agents. *Russian Journal of Bioorganic Chemistry, 41*, 192-200.

Kökbudak, Z., Akkoç, S., Karataş, H., Tüzün, B., & Aslan, G. (2022). In Silico and in vitro antiproliferative activity assessment of new schiff bases. *ChemistrySelect, 7*(3), e202103679.

Mattiuzzi, C., & Lippi, G. (2019). Current cancer epidemiology. *Journal of epidemiology and global health, 9*(4), 217-222.

Merde, I. B., Onel, G. T., Turkmenoglu, B., Gursoy, S., & Dilek, E. (2022). Pyridazinones containing the (4-methoxyphenyl)piperazine moiety as AChE/

BChE inhibitors: design, synthesis, in silico and biological evaluation. *Medicinal Chemistry Research, 31*(11), 2021-2031. doi:10.1007/s00044-022-02968-x

Murtaza, S., Akhtar, M. S., Kanwal, F., Abbas, A., Ashiq, S., & Shamim, S. (2017). Synthesis and biological evaluation of schiff bases of 4-aminophenazone as an anti-inflammatory, analgesic and antipyretic agent. *Journal of Saudi Chemical Society, 21*, S359-S372.

Önal, Z., & Yıldırım, İ. (2007). Reactions of 4-(4-methylbenzoyl)-5-(4-methylphenyl)-2, 3-furandione with semi-/thiosemi-carbazones. *Heterocyclic Communications, 13*(2-3), 113-120.

Rolland, J. S. (2005). Cancer and the family: An integrative model. *Cancer: Interdisciplinary International Journal of the American Cancer Society, 104*(S11), 2584-2595.

Schrödinger Release 2024-3: Glide, S., LLC, New York, NY, 2024.

Shaffer, D. R., Emerson, S. U., Murphy, P. C., Govindarajan, S., & Lemon, S. M. (1995). A hepatitis A virus deletion mutant which lacks the first pyrimidine-rich tract of the 5'nontranslated RNA remains virulent in primates after direct intrahepatic nucleic acid transfection. *Journal of virology, 69*(10), 6600-6604.

Shiau, A. K., Barstad, D., Loria, P. M., Cheng, L., Kushner, P. J., Agard, D. A., & Greene, G. L. (1998). The structural basis of estrogen receptor/coactivator recognition and the antagonism of this interaction by tamoxifen. *Cell, 95*(7), 927-937.

Somturk-Yilmaz, B., Altiparmak, A., Turkmenoglu, B., & Akkoc, S. (2024). Synthesis, characterization, cytotoxic activity, and molecular docking of 3, 4-diaminobenzophenone-CuhNFs and its major components-based nanoflowers. *Journal of Biomolecular Structure and Dynamics*, 1-11.

Somturk-Yilmaz, B., Turkmenoglu, B., & Akkoc, S. (2024). Synthesis, Characterization, Cytotoxic Activity Studies of N1-phenylbenzene-1, 2-diamine@ CuhNFs and 1, 2-phenylenediamine@ CuhNFs, and Molecular Docking Calculations of Their Ligands. *Journal of Inorganic and Organometallic Polymers and Materials, 34*(12), 5732-5744.

Somturk Yilmaz, B. (2024). Anticancer and Antimicrobial Activities of Quercetin-CuhNFs and Quercetin-CohNFs on MDA-MB-231 (Breast Cancer). *Journal of Inorganic and Organometallic Polymers and Materials*, 1-14.

Stamos, J., Sliwkowski, M. X., & Eigenbrot, C. (2002). Structure of the epidermal growth factor receptor kinase domain alone and in complex with a 4-anilinoquinazoline inhibitor. *Journal of Biological Chemistry, 277*(48), 46265-46272.

Türkmenoğlu, B. (2022). Investigation of novel compounds via in silico approaches of EGFR inhibitors as anticancer agents. *Journal of the Indian Chemical Society, 99*(8), 100601.

Yilmaz, B. S., Bekci, H., Altiparmak, A., Uysal, S., Şenkardeş, İ., & Zengin, G. (2024). Determination of anticancer activity and biosynthesis of Cu, Zn, and Co hybrid nanoflowers with Tribulus terrestris L. extract. *Process Biochemistry, 138*, 14-22.

Zabihollahi, R., Fassihi, A., Aghasadeghi, M. R., Memarian, H. R., Soleimani, M., & Majidzadeh-A, K. (2013). Inhibitory effect and structure–activity relationship of some Biginelli-type pyrimidines against HSV-1. *Medicinal Chemistry Research, 22*, 1270-1276.